Titanium and Zirconium Complexes That Contain the Tridentate Diamido Ligands $[(i\text{-PrN-}o\text{-}C_6H_4)_2O]^{2-}$ ($[i\text{-PrNON}]^{2-}$) and $[(C_6H_{11}N\text{-}o\text{-}C_6H_4)_2O]^{2-}$ ($[\text{CyNON}]^{2-}$)

Robert Baumann, Rüdiger Stumpf, William M. Davis, Lan-Chang Liang, and Richard R. Schrock*

Contribution from the Department of Chemistry, 6-331, Massachusetts Institute of Technology, Cambridge, Massachusetts 02139

Received October 8, 1998

Abstract: A variety of five- and six-coordinate titanium and zirconium dialkyl complexes that contain the $[(i\text{-PrN-}o\text{-}C_6H_4)_2O]^{2-}$ ($[i\text{-PrNON}]^{2-}$) ligand have been prepared, among them $[i\text{-PrNON}]Ti(CH_2CHMe_2)_2$, $[i\text{-PrNON}]Ti(CH_2CMe_3)_2$, $[i\text{-PrNON}]Zr(CH_2CH_3)_2$, and $[i\text{-PrNON}]Zr(CH_2CHMe_2)_2$. These species serve as sources of complexes such as $\{[i\text{-PrNON}]Ti(PMe_3)_2\}_2(\mu\text{-}N_2)$, $[i\text{-PrNON}]Ti(CHCMe_3)(PMe_3)_2$, $[i\text{-PrNON}]Zr(CH_2CHMe_2)_2(PMe_3)$, and $[i\text{-PrNON}]Zr(H_2C{=}CMe_2)(PMe_3)_2$. The reaction between $[i\text{-PrNON}]Ti(CH_2CMe_3)_2$ and $Me_2PCH_2CH_2PMe_2$ in the absence of dinitrogen yields $(i\text{-PrNC}_6H_4)(i\text{-PrNC}_6H_4O)Ti(dmpe)$, a pseudo-octahedral species in which one aryl−oxygen bond has been cleaved. In all structurally characterized complexes in which the $[i\text{-PrNON}]^{2-}$ ligand is intact, it adopts a *mer* configuration in which the donor oxygen atom is planar. Analogous dialkyl complexes $[\text{CyNON}]MR_2$ (Cy = cyclohexyl; M = Zr, R = Me, Et, *i*-Bu, CH_2CMe_3, allyl; M = Ti, R = Me, CH_2CMe_3, i-Bu) have also been prepared. Decomposition of $[i\text{-PrNON}]Zr(CH_2CH_3)_2$ in the absence of phosphine has been found to proceed in a first-order manner to yield $\{[i\text{-PrNON}]Zr(CH_2CH_3)\}_2(\mu\text{-}C_2H_4)$ via rate-limiting β-hydrogen abstraction to give transient $[i\text{-PrNON}]Zr(CH_2CH_2)$ followed by either intermolecular selective β-hydrogen transfer or ethyl group transfer from $[i\text{-PrNON}]Zr(CH_2CH_3)_2$ to $[i\text{-PrNON}]Zr(CH_2CH_2)$, as suggested by ^2H and ^{13}C labeling studies. Decompositions of $[i\text{-PrNON}]ZrR_2$ complexes are dramatically accelerated in the presence of PMe_3. One equivalent of PMe_3 is proposed to bind to give a pseudooctahedral adduct, $[i\text{-PrNON}]ZrR_2(PMe_3)$, in which the two alkyl (R) groups are pushed close to one another and β-hydrogen abstraction is thereby accelerated. Consistent with the relatively uncrowded coordination sphere in $[i\text{-PrNON}]^{2-}$ or $[\text{CyNON}]^{2-}$ complexes, activated dialkyls will only oligomerize 1-hexene. Compounds whose structures have been determined include $[i\text{-PrNON}]Ti(CH_2CHMe_2)_2$, $[i\text{-PrNON}]ZrMe_2$, $[i\text{-PrNON}]Zr(H_2C{=}CHMe_2)_2(PMe_3)$, $[i\text{-PrNON}]Zr(CH_2CMe_2)(PMe_3)_2$, $[i\text{-PrNON}]Ti(PMe_3)_2]_2(\mu\text{-}N_2)$, $[i\text{-PrNON}]Ti(CHCMe_3)(PMe_3)_2$, and $(i\text{-PrNC}_6H_4)(i\text{-PrNC}_6H_4O)Ti(dmpe)$.

Introduction

We recently reported the synthesis of titanium, zirconium, and hafnium complexes that contain the $[(t\text{-BuN-}o\text{-}C_6H_4)_2O]^{2-}$ ($[t\text{-BuNON}]^{2-}$) ligand, and the living polymerization of up to ~1000 equiv of 1-hexene by activated zirconium dimethyl complexes in chlorobenzene at 0 °C.[1−3] All five-coordinate compounds, e.g., $[t\text{-BuNON}]ZrMe_2$ and the $B(C_6F_5)_3$-activated zirconium dimethyl complex, were shown to be "twisted", approximately trigonal bipyramidal species in which the amido nitrogens occupy *equatorial* positions and the two R′ groups are inequivalent (a "twisted *fac*" structure; eq 1). However, the

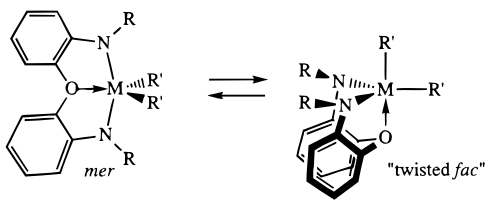

(1)

two R′ groups equilibrate rapidly on the NMR time scale in solution, even at −80 °C, presumably via a *mer* structure with C_2 or C_{2v} symmetry. We began to suspect that the *mer* structure is the higher energy species when R = *t*-Bu because of steric interaction between the *tert*-butyl group and the two equatorial R′ groups, that a twisted *fac* structure for the dimethyl complex is a predictor of steric crowding in a pseudotetrahedral cationic monoalkyl complex, and that a four-coordinate cationic monoalkyl species will more likely behave as a living catalyst for polymerization of ordinary olefins if the twisted *fac* structure is the lower energy species. We set out to test this theory by preparing analogous complexes in which the R group is isopropyl or cyclohexyl. We have found that only *mer* structures are observed in a variety of five-coordinate (and six-coordinate) titanium and zirconium complexes that contain the $[(i\text{-PrN-}o\text{-}C_6H_4)_2O]^{2-}$ ($[i\text{-PrNON}]^{2-}$) ligand, consistent with a natural preference for twisted *mer* structures in the sterically less demanding circumstance. We have also found that "$\{[i\text{-PrNON}]ZrMe\}[B(C_6F_5)_4]$" will only oligomerize 1-hexene, consistent with the metal center not being sufficiently crowded, and perhaps far from pseudotetrahedral.

(1) Baumann, R.; Davis, W. M.; Schrock, R. R. *J. Am. Chem. Soc.* **1997**, *119*, 3830.
(2) Baumann, R.; Schrock, R. R. *J. Organomet. Chem.* **1998**, *557*, 69.
(3) Schrock, R. R.; Baumann, R.; Reid, S. M.; Goodman, J. T.; Stumpf, R.; Davis, W. M. *Organometallics*, in press.

10.1021/ja983549v CCC: $18.00
Published on Web 08/11/1999

Results

Synthesis of Ti and Zr [(*i*-PrNC$_6$H$_4$)$_2$O]$^{2-}$ Complexes. The isopropyl derivative of (NH$_2$-*o*-C$_6$H$_4$)$_2$O, [(*i*-PrNHC$_6$H$_4$)$_2$O] (H$_2$-[*i*-PrNON]), can be prepared readily from acetone and zinc in acetic acid, and isolated as a pale yellow oil in high yield on a ~10 g scale. This methodology is derived from that reported for the synthesis of a variety of substituted anilines.[4]

Addition of 2 equiv of LiBu to a solution of H$_2$[*i*-PrNON] in ether, followed by addition of (NMe$_2$)$_2$TiCl$_2$, yielded the dimethylamido complex [*i*-PrNON]Ti(NMe$_2$)$_2$, an orange oil that was used in crude form for further reactions. Proton NMR spectra of [*i*-PrNON]Ti(NMe$_2$)$_2$ suggest that it has C_{2v} symmetry on the NMR time scale; only one singlet at ~3.1 ppm for the dimethylamido groups is observed, and the isopropyl methyl groups are equivalent. The dichloride complex [*i*-PrNON]TiCl$_2$ was obtained quantitatively in 24 h by treating [*i*-PrNON]Ti-(NMe$_2$)$_2$ with Me$_3$SiCl (eq 2). [*i*-PrNON]TiCl$_2$ is a deep purple-

$$(NMe_2)_2TiCl_2 \xrightarrow[\text{ether, } -25\ ^\circ\text{C}]{\text{Li}_2[i\text{-PrNON}]} [i\text{-PrNON}]Ti(NMe_2)_2 \xrightarrow[\text{toluene, } 110\ ^\circ\text{C}]{2Me_3SiCl} [i\text{-PrNON}]TiCl_2 \quad (2)$$

black solid that is moderately soluble in toluene and ether. A possible dimeric structure for [*i*-PrNON]TiCl$_2$ with bridging chlorides cannot be ruled out on the basis of the observed dimeric structure for [*t*-BuNON]ZrCl$_2$.[3]

Alkylation of [*i*-PrNON]TiCl$_2$ with 2 equiv of MeMgI, Me$_2$CHCH$_2$MgCl, or Me$_3$CCH$_2$MgCl yielded the corresponding dialkyl complexes (eq 3) as orange microcrystalline solids in

$$[i\text{-PrNON}]TiCl_2 \xrightarrow{2RMgX,\ -25\ ^\circ\text{C}} [i\text{-PrNON}]TiR_2 \quad (3)$$

$$R = Me,\ CH_2CHMe_2,\ \text{or}\ CH_2CMe_3$$

51−69% yields. At room temperature the ^{1}H NMR spectra of [*i*-PrNON]TiR$_2$ complexes are consistent with their having C_{2v} symmetry on the NMR time scale in solution. [*i*-PrNON]Ti-(CH$_2$CHMe$_2$)$_2$ can be stored as a solid at −25 °C, but it slowly decomposes at room temperature within ~1 day to a mixture of unidentified products. [*i*-PrNON]Ti(CH$_2$CMe$_3$)$_2$ is relatively stable in the solid state at 22 °C, but it is best stored at −25 °C. In C$_6$D$_6$ solution [*i*-PrNON]Ti(CH$_2$CMe$_3$)$_2$ decomposes completely within 12 h at 50 °C to unidentified products. Attempts to prepare and isolate [*i*-PrNON]Ti-(CH$_2$CH$_3$)$_2$ failed.

The zirconium dichloride complex [*i*-PrNON]ZrCl$_2$ was prepared via the route shown in eq 4. Dialkyl complexes

$$H_2[i\text{-PrNON}] + Zr(NMe_2)_4 \xrightarrow{-2Me_2NH} [i\text{-PrNON}]Zr(NMe_2)_2 \xrightarrow{\text{excess } Me_3SiCl} [i\text{-PrNON}]ZrCl_2 \xrightarrow{\text{alkylation}} [i\text{-PrNON}]ZrR_2 \quad (4)$$

$$R = Me,\ Et,\ i\text{-Bu},\ CH_2CMe_3$$

[*i*-PrNON]ZrR$_2$, where R = Me, Et, CH$_2$CHMe$_2$, or CH$_2$CMe$_3$, could all be prepared in a straightforward manner. The [*i*-PrNON]ZrEt$_2$ complex is the least stable toward β-hydrogen abstraction, as one would predict on the basis of studies involving zirconocene dialkyl complexes;[5,6] decomposition studies are described in detail in a later section. It is interesting

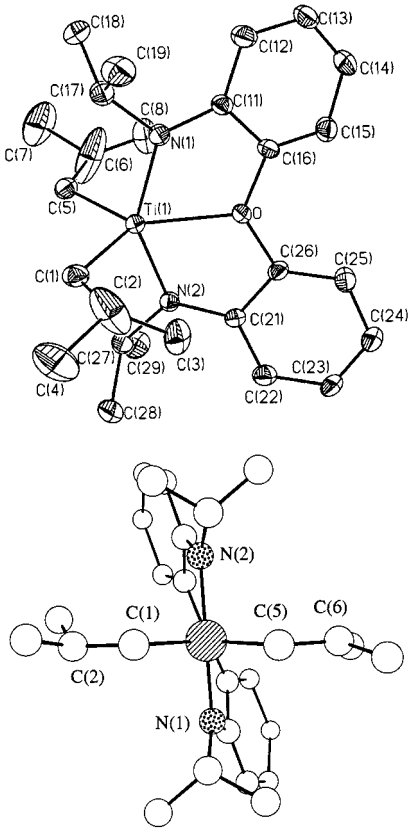

Figure 1. (a, top) ORTEP diagram (35% probability level) of [*i*-PrNON]Ti(CH$_2$CHMe$_2$)$_2$. (b, bottom) Chem 3D drawing of [*i*-PrNON]-Ti(CH$_2$CHMe$_2$)$_2$.

to note that [*i*-PrNON]Zr(CH$_2$CHMe$_2$)$_2$ can be prepared directly from ZrCl$_4$ in good yield (eq 5). We believe that the product of

$$ZrCl_4 \xrightarrow[\text{2. } 4i\text{-BuMgCl, } -25\ ^\circ\text{C, 30 min}]{\text{1. } H_2[i\text{-PrNON}],\ \text{toluene, 22 °C, 5 h}} [i\text{-PrNON}]Zr(CH_2CHMe_2)_2 \quad (5)$$

the reaction between ZrCl$_4$ and H$_2$[*i*-PrNON] is an adduct, subsequent dehydrochlorination and alkylation of which by the Grignard reagent proceed smoothly to give [*i*-PrNON]Zr-(CH$_2$CHMe$_2$)$_2$ in a 60% isolated yield on a 1−2 g scale.

The structure of [*i*-PrNON]Ti(CH$_2$CHMe$_2$)$_2$, as determined in a single-crystal X-ray study, is a distorted trigonal bipyramid, as shown in Figure 1. (See also Tables 1 and 3.) The [*i*-PrNON]$^{2-}$ ligand is coordinated in a meridional manner with oxygen in the equatorial position and the planar amido nitrogens in the "axial" positions with a N(1)−Ti−N(2) angle of 145.53-(14)°. The *mer* configuration is best characterized by an angle between the N(1)/Ti/O and N(2)/Ti/O planes of 180°. The two isobutyl groups are found in equatorial positions, with the C(1)−Ti−C(5) angle being 104.6(2)°. The [*i*-PrNON]$^{2-}$ ligand backbone is twisted (Figure 1b), as shown by O−Ti−N−C$_{i-Pr}$ dihedral angles of 172.0° and 168.7°, in part to minimize unfavorable steric interactions between the hydrogen atoms ortho to the oxygen atom, but also in part as a consequence of the inflexible nature of the *o*-phenylene backbone. The Ti−O distance is 2.149(3) Å, and the oxygen atom is planar. The Ti−O$_{donor}$ distance contrasts with the relatively long Ti−O$_{donor}$ bond

(4) Micovic, I. V.; Ivanovic, M. D.; Piatak, D. M.; Bojic, V. D. *Synthesis* **1991**, 1043.

(5) Negishi, E.; Takahashi, T. *Acc. Chem. Res.* **1994**, *27*, 124.

(6) Negishi, E.; Nguyen, T.; Maye, J. P.; Choueiri, D.; Suzuki, N.; Takahashi, T. *Chem. Lett.* **1992**, 2367.

Table 1. Crystal Data and Structure Refinement for [*i*-PrNON]Ti(CH_2CHMe_2)$_2$, [*i*-PrNON]Ti(PMe_3)$_2$]$_2$(μ-N_2), (*i*-PrNC_6H_4)(*i*-PrNC_6H_4O)Ti(dmpe), and [*i*-PrNON]Ti($CHCMe_3$)(PMe_3)$_2$ (L = [*i*-PrNON]$^{2-}$)

compound	$LTi(CH_2CHMe_2)_2$	$[LTi(PMe_3)_2]_2(\mu\text{-}N_2)$	(*i*-PrNC_6H_4)(*i*-PrNC_6H_4O)Ti(dmpe)	$LTi(CHCMe_3)(PMe_3)_2$
crystals obtained from	pentane	ether	toluene/pentane	toluene/pentane
formula	$C_{26}H_{40}N_2OTi$	$C_{48}H_{80}N_6O_2P_4Ti_2$	$C_{24}H_{38}N_2OP_2Ti$	$C_{29}H_{50}N_2OP_2Ti$
formula weight	444.50	992.86	480.40	552.55
crystal size (mm)	0.18 × 0.12 × 0.08	0.23 × 0.16 × 0.12	0.32 × 0.28 × 0.25	0.38 × 0.12 × 0.12
crystal system	triclinic	orthorhombic	monoclinic	monoclinic
space group	$P\bar{1}$	*Pbcn*	*C*2/*c*	$P2_1/c$
a (Å)	9.14700(10)	22.2673(7)	36.7261(13)	16.3753(8)
b (Å)	10.0436(3)	13.6674(5)	10.3024(4)	17.2240(9)
c (Å)	14.2372(4)	19.6101(6)	14.7015(5)	11.5092(6)
α (deg)	79.552(2)	90	90	90
β (deg)	88.5520(10)	90	109.88	96.9710(10)
γ (deg)	77.869(2)	90	90	90
V (Å^3)	1257.43(5)	5968.1(3)	5231.2(3)	3222.2(3)
Z	2	4	8	4
density calcd (Mg/m^3)	1.174	1.105	1.220	1.139
μ (mm^{-1})	0.359	0.412	0.467	0.387
F (000)	480	2120	2048	1192
T (K)	183(2)	183(2)	190(2)	193(2)
θ range (ω scans)	1.45−23.24°	1.75−20.00°	2.06−23.25°	1.25−23.26°
no. of reflections collected	5146	16332	10398	12888
no. of independent reflections	3527	2785	3754	4613
no. of data/restr/parameters	3524/0/290	2781/0/281	3748/0/272	4603/0/344
goodness-of-fit on F^2	1.063	1.125	1.046	0.900
*R*1/*wR*2 [$I > 2\sigma(I)$]	0.0561/0.1408	0.0598/0.1690	0.0443/0.1060	0.0521/0.1374
*R*1/*wR*2 (all data)	0.0832/0.1846	0.0660/0.1829	0.0594/0.1213	0.0786/0.1762
extinction coefficient	0.008(3)	0.0036(6)	0.00003(8)	0.0089(12)
max/min peaks (e/Å^3)	0.332/−0.345	0.499/−0.357	0.420/−0.264	0.350/−0.355

Table 2. Crystal Data and Structure Refinement for [*i*-PrNON]$ZrMe_2$, [*i*-PrNON]Zr(CH_2CHMe_2)$_2$(PMe_3), and [*i*-PrNON]Zr(η^2-CH_2CMe_2)(PMe_3)$_2$ ([*i*-PrNON]$^{2-}$ = L)

compound	$LZrMe_2$	$LZr(CH_2CHMe_2)_2(PMe_3)$	$LZr(CH_2CMe_2)(PMe_3)_2$
crystals obtained from	pentane	pentane	toluene/pentane/PMe_3
formula	$C_{20}H_{28}N_2OZr$	$C_{29}H_{49}N_2OPZr$	$C_{28}H_{48}N_2OP_2Zr$
formula weight	403.66	563.89	581.84
crystal size (mm)	0.38 × 0.12 × 0.12	0.38 × 0.25 × 0.22	0.32 × 0.08 × 0.08
crystal system	orthorhombic	triclinic	monoclinic
space group	$P2_12_12_1$	$P\bar{1}$	$P2_1/n$
a (Å)	8.415(2)	9.8443(2)	10.5432(3)
b (Å)	13.889(3)	9.91370(10)	21.6042(5)
c (Å)	16.544(4)	16.40460(10)	13.2855(2)
α (deg)	90	90.0120(10)	90
β (deg)	90	97.0780(10)	93.5560(10)
γ (deg)	90	101.6160(10)	90
V (Å^3)	1933.6(8)	1555.73(4)	3020.31(12)
Z	4	2	4
density calcd (Mg/m^3)	1.387	1.204	1.280
μ (mm^{-1})	0.577	0.426	0.492
F (000)	840	600	1232
T (K)	183(2)	293(2)	183(2)
θ range (ω scans)	1.91−23.26°	1.25−23.24°	1.80−20.00°
no. of reflections collected	7753	6414	8975
no. of independent reflections	2771	4354	2815
data/restraints/parameters	2771/0/218	4350/0/308	2622/0/308
goodness-of-fit on F^2	1.164	1.010	1.047
*R*1/*wR*2 [$I > 2\sigma(I)$]	0.0323/0.0655	0.0409/0.1097	0.0409/0.0787
*R*1/*wR*2 (all data)	0.0363/0.0667	0.0529/0.1345	0.0658/0.1120
extinction coefficient	0.0027(5)	0.008(2)	0.0007(2)
max/min peaks (e/Å^3)	0.409/−0.533	0.385/−0.614	0.453/−0.343

length (2.402(4) Å) found in [*t*-BuNON]$TiMe_2$, which has the *fac* geometry in the solid state.[3]

The solid-state structure of [*i*-PrNON]$ZrMe_2$ is similar to that of [*i*-PrNON]Ti(CH_2CHMe_2)$_2$ (Figure 2, Tables 2 and 3). The larger size of Zr accounts for the longer metal−ligand bonds in [*i*-PrNON]$ZrMe_2$ than in [*i*-PrNON]Ti(CH_2CHMe_2)$_2$, and also for the slightly smaller N−Zr−N angle (137.70(12)°) relative to the N−Ti−N angle (145.53(14)°). The M−N−C_{i-Pr} angle in [*i*-PrNON]$ZrMe_2$ is also 6−7° smaller than it is in [*i*-PrNON]-Ti(CH_2CHMe_2)$_2$. The O−M−N−C_{i-Pr} dihedral angles in [*i*-PrNON]$ZrMe_2$ are close to 180°, perhaps largely as a consequence of the lower degree of steric crowding in the zirconium complex between the amido isopropyl groups and the equatorial alkyl groups. The Zr−O_{donor} distance (2.309(2) Å) is ∼0.1 Å shorter than in [*t*-BuNON]$ZrMe_2$ (2.418(3) Å),[3] consistent with more efficient M−O bonding in the *mer* structure, perhaps in part as a consequence of some Zr−O π bonding.

Both titanium and zirconium dialkyl complexes appear to be sensitive to light, even fluorescent room light, especially in the presence of phosphines. In several cases (see below) reactions involving phosphines that were not protected from room light were compromised to a significant degree by side reactions.

Table 3. Selected Bond Lengths (Å) and Angles (deg) in [*i*-PrNON]Ti(CH_2CHMe_2)$_2$, [*i*-PrNON]ZrMe_2, and [*i*-PrNON]Zr(CH_2CHMe_2)$_2$(PMe_3)

[*i*-PrNON]Ti(CH_2CHMe_2)$_2$		[*i*-PrNON]ZrMe_2		[*i*-PrNON]Zr(CH_2CHMe_2)$_2$(PMe_3)	
Ti−O	2.149(3)	Zr−O	2.309(2)	Zr−O	2.329(2)
Ti−N(1)	1.993(3)	Zr−N(1)	2.087(3)	Zr−N(1)	2.107(3)
Ti−N(2)	1.993(3)	Zr−N(2)	2.087(3)	Zr−N(2)	2.113(3)
Ti−C(5)	2.106(4)	Zr−C(2)	2.243(4)	Zr−C(1)	2.280(3)
Ti−C(1)	2.099(4)	Zr−C(1)	2.237(4)	Zr−C(5)	2.268(4)
N(1)−Ti−N(2)	145.53(14)	N(1)−Zr−N(2)	137.70(12)	N(1)−Zr−N(2)	137.27(12)
N(1)−Ti−O	72.66(12)	N(1)−Zr−O	69.07(10)	N(1)−Zr−O	69.51(10)
N(1)−Ti−C(5)	97.2(2)	N(1)−Zr−C(2)	101.53(13)	N(1)−Zr−C(1)	113.83(12)
N(1)−Ti−C(1)	103.8(2)	N(1)−Zr−C(1)	101.40(14)	N(1)−Zr−C(5)	93.95(12)
N(2)−Ti−O	72.87(12)	N(2)−Zr−O	68.80(11)	N(2)−Zr−O	68.76(10)
N(2)−Ti−C(5)	103.8(2)	N(2)−Zr−C(2)	101.99(13)	N(2)−Zr−C(1)	104.62(13)
N(2)−Ti−C(1)	97.0(2)	N(2)−Zr−C(1)	102.42(14)	N(2)−Zr−C(5)	99.13(13)
C(5)−Ti−O	127.9(2)	C(2)−Zr−O	129.5(2)	C(1)−Zr−O	154.69(12)
C(5)−Ti−C(1)	104.6(2)	C(2)−Zr−C(1)	110.7(2)	C(5)−Zr−C(1)	97.33(13)
C(1)−Ti−O	127.5(2)	C(1)−Zr−O	119.81(13)	C(5)−Zr−O	107.77(12)
C(16)−O−C(26)	125.8(3)	C(16)−O−C(26)	125.3(3)	C(12)−O−C(22)	125.9(3)
Ti−N(1)−C(17)	117.6(3)	Zr−N(1)−C(17)	111.5(2)	Zr−N(1)−C(17)	112.1(2)
Ti−N(2)−C(27)	117.9(3)	Zr−N(2)−C(27)	110.3(2)	Zr−N(2)−C(27)	114.8(2)
N(1)/Ti/O/N(2)[a,b]	180	N(1)/Zr/O/N(2)[a,b]	176	N(1)/Zr/O/N(2)[a,b]	180
O−Ti−N(1)−C(17)[a]	172.0	O−Zr−N(1)−C(17)[a]	178.8	O−Zr−N(1)−C(17)[a]	177.5
O−Ti−N(2)−C(27)[a]	168.7	O−Zr−N(2)−C(27)[a]	176.0	O−Zr−N(2)−C(27)[a]	166.4
				Zr−P	3.0326(11)
				P−Zr−C(5)	174.44(10)
				P−Zr−C(1)	77.78(9)

[a] Obtained from a Chem 3D model. [b] The external angle between the planes.

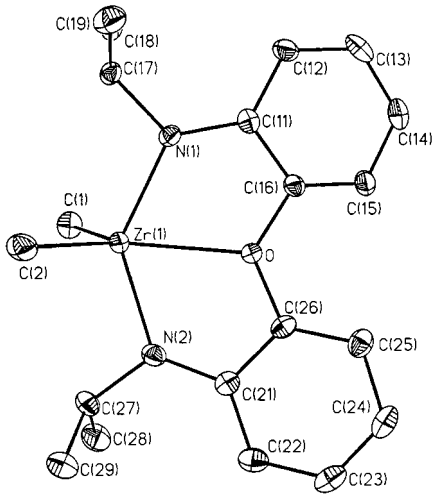

Figure 2. ORTEP diagram (35% probability level) of [*i*-PrNON]-ZrMe_2.

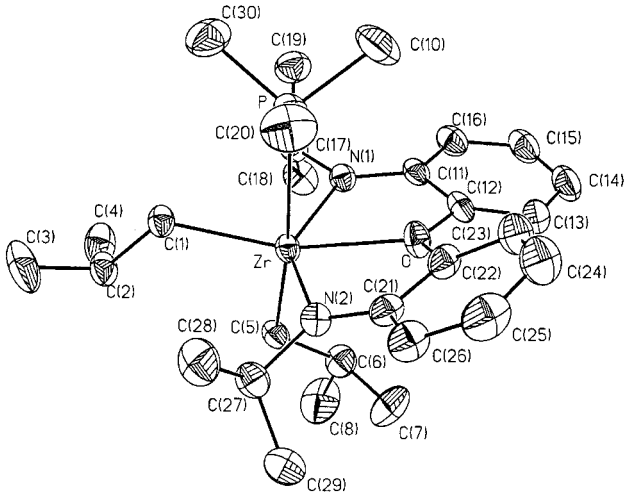

Figure 3. ORTEP diagram (35% probability level) of [*i*-PrNON]Zr-(CH_2CHMe_2)$_2$(PMe_3).

All attempts to characterize the decomposition product or products of photochemical decomposition reactions failed, even in the presence of a phosphine such as PMe_3 (see below).

Decomposition of [*i*-PrNON]Zr(CH_2CHMe_2)$_2$ in the Presence of PMe_3. Upon addition of PMe_3 to a C_6D_6 solution of [*i*-PrNON]Zr(CH_2CHMe_2)$_2$ a downfield shift of the isobutyl methyl resonances is observed in the ^{1}H NMR spectrum. A variable-temperature ^{31}P NMR study of a toluene-d_8 solution of [*i*-PrNON]Zr(CH_2CHMe_2)$_2$ in the presence of PMe_3 (∼3 equiv) reveals one sharp singlet at −59.3 ppm at room temperature. At −80 °C two broad resonances appear, one at −49.2 ppm for coordinated PMe_3, and the other at −61.7 ppm for free PMe_3. Upon cooling a pentane solution of [*i*-PrNON]Zr-(CH_2CHMe_2)$_2$ to −25 °C in the presence of excess PMe_3, pale yellow crystals formed whose elemental analysis is consistent with the formulation [*i*-PrNON]Zr(CH_2CHMe_2)$_2$(PMe_3). Proton and ^{31}P NMR spectra of [*i*-PrNON]Zr(CH_2CHMe_2)$_2$(PMe_3) confirm that proposal. However, the spectra are concentration and temperature dependent and consistent with ready loss of PMe_3 to yield [*i*-PrNON]Zr(CH_2CHMe_2)$_2$.

An X-ray study of a single crystal of [*i*-PrNON]Zr-(CH_2CHMe_2)$_2$(PMe_3) (Tables 2 and 3) revealed the pseudooctahedral structure shown in Figure 3. The PMe_3 has attacked the metal from "outside" the C−Zr−C wedge and in the ZrC_2 plane (eq 6). The Zr−P bond length is quite long (3.0326(11)

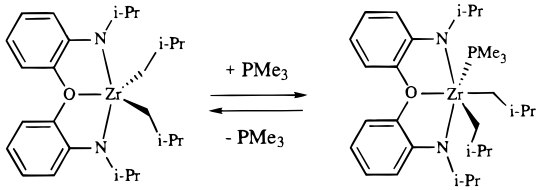

(6)

Å), consistent with the relatively crowded pseudooctahedral environment and lability of the PMe_3 ligand. The [*i*-PrNON]$^{2-}$ ligand is coordinated in a twisted *mer* fashion (N(1)/Zr/O/N(2)

Table 4. Selected Bond Lengths (Å) and Angles (deg) in [*i*-PrNON]Zr(CH_2CMe_2)(PMe_3)$_2$, {[*i*-PrNON]Ti(PMe_3)$_2$}$_2$(μ-N_2), [*i*-PrNON]Ti($CHCMe_3$)(PMe_3)$_2$

[*i*-PrNON]Zr(CH_2CMe_2)(PMe_3)$_2$		{[*i*-PrNON]Ti(PMe_3)$_2$}$_2$(μ-N_2)		[*i*-PrNON]Ti($CHCMe_3$)(PMe_3)$_2$	
Zr−O	2.367(3)	Ti−O	2.198(3)	Ti−O	2.202(3)
Zr−N(1)	2.170(4)	Ti−N(1)	2.068(4)	Ti−N(1)	2.080(3)
Zr−N(2)	2.161(4)	Ti−N(2)	2.123(4)	Ti−N(2)	2.074(3)
N(1)−Zr−O	68.48(14)	N(1)−Ti−O	72.40(13)	N(1)−Ti−O	72.81(11)
N(2)−Zr−O	68.26(14)	N(2)−Ti−O	72.44(13)	N(2)−Ti−O	72.44(10)
N(1)−Zr−N(2)	136.7(2)	N(1)−Ti−N(2)	144.6(2)	N(2)−Ti−N(1)	145.22(13)
Zr−N(1)−C(17)	118.8(3)	Ti−N(1)−C(111)	121.2(3)	C(17)−N(1)−Ti	122.8(3)
Zr−N(2)−C(27)	120.7(3)	Ti−N(2)−C(210)	130.4(4)	C(27)−N(2)−Ti	122.7(2)
C(11)−O−C(21)	126.8(4)	C(11)−O−C(21)	126.5(4)	C(11)−O−C(26)	128.3(3)
N(1)/Zr/O/N(2)[a,b]	178	N(1)/Ti/O/N(2)[a,b]	176	N(1)/Ti/O/N(2)[a,b]	179
O−Zr−N(1)−C(17)[b]	162.8	O−Ti−N(1)−C(111)[b]	165.9	O−Ti−N(1)−C(17)[b]	162.6
O−Zr−N(2)−C(27)[b]	159.6	O−Ti−N(2)−C(210)[b]	171.1	O−Ti−N(2)−C(27)[b]	166.1
Zr−C(2)	2.291(6)	Ti−N(3)	1.811(4)	Ti−C(1)	1.884(4)
Zr−P(2)	2.790(2)	Ti−P(2)	2.650(2)	Ti−P(1)	2.6368(12)
Zr−P(3)	2.803(2)	Ti−P(3)	2.668(2)	Ti−P(2)	2.6396(12)
C(1)−C(2)	1.457(8)	Ti−N(3)−N(3A)	177.7(4)	C(2)−C(1)−Ti	179.3(3)
P(2)−Zr−P(3)	160.55(5)	P(2)−Ti−P(3)	166.69(5)	P(1)−Ti−P(2)	169.42(4)
N(1)−Zr−C(2)	111.8(2)	N(3)−Ti−O	175.5(2)	C(1)−Ti−N(2)	106.83(14)
N(1)−Zr−C(1)	110.2(2)	N(3)−N(3A)	1.264(8)	C(1)−Ti−N(1)	107.95(15)
N(2)−Zr−C(2)	108.1(2)			C(1)−Ti−P(1)	94.85(12)
N(2)−Zr−C(1)	111.7(2)			C(1)−Ti−O	178.20(14)
C(2)−Zr−O	159.7(2)			N(2)−Ti−P(1)	87.01(9)
C(2)−Zr−C(1)	36.8(2)			N(1)−Ti−P(1)	89.72(9)
C(1)−Zr−O	163.5(2)			O−Ti−P(1)	86.78(8)
Zr−C(1)	2.327(5)			C(1)−Ti−P(2)	95.73(12)
				N(2)−Ti−P(2)	89.87(9)
				N(1)−Ti−P(2)	87.09(9)
				O−Ti−P(2)	82.64(8)

[a] The external angle between the planes. [b] Obtained from a Chem 3D model.

= 180°), similar to what is found in [*i*-PrNON]Ti(CH_2CHMe_2)$_2$ and [*i*-PrNON]ZrMe_2. Metal−ligand bond lengths are all slightly longer (by ∼0.02−0.04 Å) than they are in [*i*-PrNON]ZrMe_2, consistent with more steric crowding and greater electron donation to the metal in the six-coordinate species. Coordination of PMe_3 forces the two isobutyl groups together (C(1)−Zr−C(5) = 97.33(13)°), but the weak coordination of PMe_3 and repulsion between the two isobutyl groups prevent a further decrease in the C−Zr−C angle. The isobutyl group cis to PMe_3 turns away from PMe_3, while the isobutyl group containing C(5) turns away from that containing C(1), so that C(6) is oriented toward the relatively open face of the [*i*-PrNON]$^{2-}$ ligand. It is tempting to propose that in the β-hydrogen abstraction reaction described below the proton on C(2) is transferred to carbon atom C(5), which is 2.93 Å away from it. The Zr−C(1) and Zr−C(5) distances are essentially equal, giving no hint as to which is the weaker Zr−C bond.

When a solution of [*i*-PrNON]Zr(CH_2CHMe_2)$_2$ in neat PMe_3 is heated to 37 °C, the isobutylene adduct [*i*-PrNON]Zr(η^2-CH_2CMe_2)(PMe_3)$_2$ is formed and can be isolated in ∼59% yield (eq 7). The reaction must be performed in the absence of light;

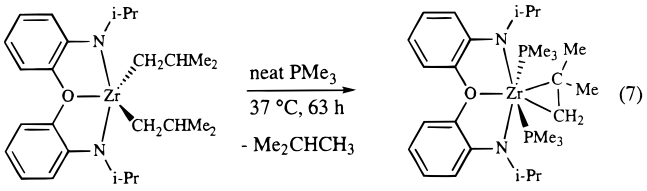

(7)

otherwise the sample decomposes to unidentified products. Room temperature ^{31}P NMR spectra (in C_6D_6) of [*i*-PrNON]Zr(η^2-CH_2CMe_2)(PMe_3)$_2$ show two broad PMe_3 resonances at −26.0 ppm (coordinated PMe_3) and −60.1 ppm (free PMe_3), consistent with ready loss of one PMe_3 from [*i*-PrNON]Zr(η^2-CH_2CMe_2)(PMe_3)$_2$. The isopropyl methyl groups are diastereotopic, whereas the isopropyl methine protons are equivalent, indicating that the molecule has C_s symmetry on the NMR time scale. While C_6D_6 solutions of [*i*-PrNON]Zr(η^2-CH_2CMe_2)(PMe_3)$_2$ are stable in solution at room temperature for several hours, significant decomposition is observed at 40 °C. Solutions of [*i*-PrNON]Zr(η^2-CH_2CMe_2)(PMe_3)$_2$ that contain additional PMe_3 are significantly more stable. Apparently [*i*-PrNON]Zr(η^2-CH_2CMe_2)(PMe_3) is not stable enough to be isolated.

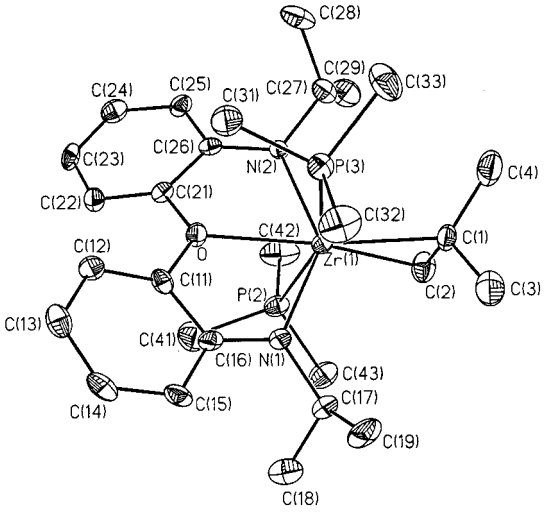

Figure 4. ORTEP diagram (35% probability level) of [*i*-PrNON]Zr(η^2-CH_2CMe_2)(PMe_3)$_2$.

An X-ray study of [*i*-PrNON]Zr(η^2-CH_2CMe_2)(PMe_3)$_2$ (Tables 2 and 4) confirms that the phosphines are coordinated trans to one another (P(2)−Zr−P(3) = 160.55(5)°) and the isobutylene ligand is coordinated trans to the oxygen donor of the [*i*-PrNON]$^{2-}$ ligand (Figure 4). The Zr−P bonds are shorter than the Zr−P bond in [*i*-PrNON]Zr(CH_2CHMe_2)$_2$(PMe_3), although still relatively long, consistent with a crowded pseu-

dooctahedral complex. The [*i*-PrNON]$^{2-}$ ligand adopts the *mer* conformation with bond lengths and angles similar to those found in [*i*-PrNON]Zr(CH_2CHMe_2)$_2$(PMe_3). The Zr−C(1) distance (2.327(5) Å) is slightly longer than Zr(1)−C(2) (2.291(6) Å), which is what one would expect on steric grounds, and what has been observed in $Cp_2Hf(\eta^2$-$CH_2CMe_2)(PMe_3)$.[7] The C(1)−C(2) bond length (1.457(8) Å) is consistent with a substantial degree of back-bonding into the olefin. It should be noted that the two olefinic carbon atoms of the coordinated isobutylene in [*i*-PrNON]Zr(η^2-CH_2CMe_2)(PMe_3)$_2$ lie almost in the ZrP_2 plane, in contrast to the twisting of the ethylene in [*t*-BuNON]Zr(η^2-CH_2CH_2)(PMe_3)$_2$ ∼15° out of the ZrP_2 plane.[3] These facts are consistent with a greatly reduced steric influence by the isopropyl groups in comparison with *tert*-butyl groups in complexes of this general type. NMR spectra of [*i*-PrNON]Zr(η^2-CH_2CMe_2)(PMe_3)$_2$ are consistent with no ready rotation of the isobutylene ligand about the Zr−O axis by ∼90°, which would generate a second mirror plane in the molecule and equilibrate the isopropyl methyl groups; the more facile process is loss of one PMe_3 ligand. The PMe_3 ligand next to C(1) on steric grounds would appear to be the one that is lost most readily.

Addition of trimethylphosphine to [*i*-PrNON]$ZrPr_2$ and [*i*-PrNON]$ZrEt_2$ led to quantitative formation of [*i*-PrNON]Zr(η^2-CH_2CHCH_3)(PMe_3)$_2$ and [*i*-PrNON]Zr(η^2-CH_2CH_2)(PMe_3)$_2$, respectively, according to NMR studies. The isopropyl methyl groups are all inequivalent in the former, as they must be regardless of whether propylene rotates rapidly about the Zr−propylene bond axis or not.

Decomposition Reactions of Titanium Dialkyl Complexes. Decomposition of [*i*-PrNON]Ti(CH_2CHMe_2)$_2$ in the presence of PMe_3 (∼4 equiv) under dinitrogen (1 atm) yields the bridging dinitrogen complex {[*i*-PrNON]Ti(PMe_3)$_2$}$_2$(μ-N_2) in 61% isolated yield (eq 8). We propose that trimethylphosphine

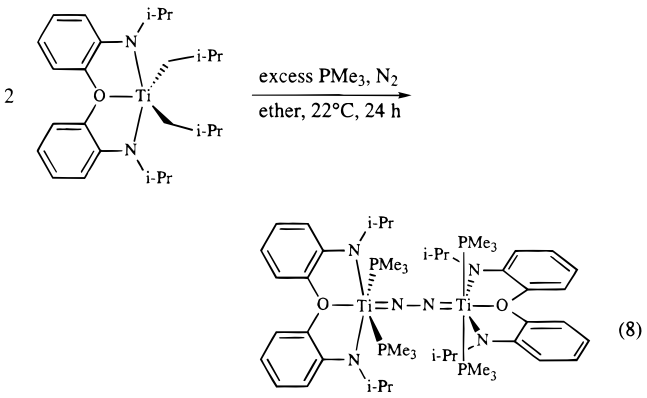

induces decomposition of [*i*-PrNON]Ti(CH_2CHMe_2)$_2$ to yield isobutane and an intermediate isobutene complex, [*i*-PrNON]Ti(η^2-CH_2CMe_2)(PMe_3). The isobutene complex then loses isobutene and binds dinitrogen, and another equivalent of PMe_3 adds to yield the observed product.

An X-ray structure of {[*i*-PrNON]Ti(PMe_3)$_2$}$_2$(μ-N_2) (Tables 1 and 4, Figure 5) confirms that two identical pseudooctahedral titanium fragments are linearly bridged by one dinitrogen molecule (Ti(1)−N(3)−N(3A) = 177.7(4)°) and twisted with respect to one another by 90°. The geometry about the one unique titanium center can be described as distorted octahedral with two PMe_3 molecules mutually trans and the titanium atom lying in the N−O−N plane. The dinitrogen could be said to be

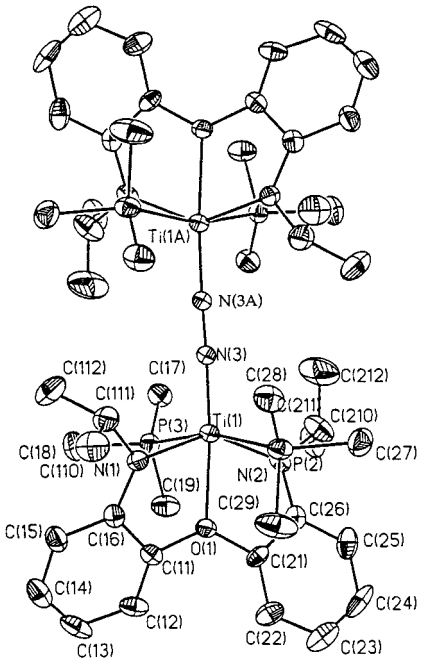

Figure 5. ORTEP diagram (35% probability level) of {[*i*-PrNON]Ti(PMe_3)$_2$}$_2$(μ-N_2).

a "hydrazido^{4-}" type,[8,9] according to the N−N bond distance of 1.264(8) Å and a Ti−N(3) distance of 1.811(4) Å. The Ti−(μ-N_2) bond distance (Ti(1)−N(3) = 1.811(4) Å) and the N−N bond distance (N(3)−N(3A) = 1.264(8) Å) are similar to distances in titanium dinitrogen complexes that contain nitrogen-based ancillary ligands.[10−12] Titanium(II) dinitrogen complexes stabilized by cyclopentadienyl ligands[13−15] have longer Ti−N bonds (1.920−2.033 Å) and shorter N−N (1.155−1.191 Å) bonds, consistent with less reduction of dinitrogen and less electron delocalization across the dinitrogen bridge. The [*i*-PrNON]$^{2-}$ ligand adopts the same twisted *mer* configuration that is found in other complexes reported here.

When [*i*-PrNON]Ti(CH_2CHMe_2)$_2$ was allowed to decompose in benzene in the presence of DMPE ($Me_2PCH_2CH_2PMe_2$) and in the absence of dinitrogen in the dark at 22 °C, the color of the reaction mixture changed from bright orange to red-black. Black crystals of the new diamagnetic complex appeared to have the formula [*i*-PrNON]Ti(dmpe), according to elemental analyses. However, the complex proton and carbon NMR spectra suggested that the molecule had no symmetry. An X-ray study revealed that "[*i*-PrNON]Ti(dmpe)" is formally the product of an oxidative addition of an *aryl*−*oxygen* bond of the ligand backbone (C(26)−O(1)) to the metal center (eq 9, Tables 1 and

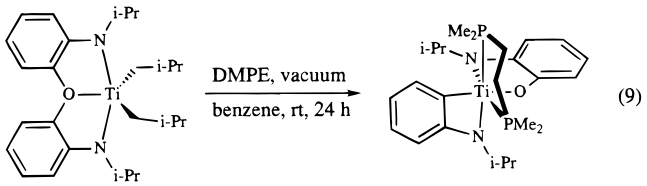

5, Figure 6); O(1) and C(26) end up approximately trans to one

(7) Buchwald, S. L.; Kreutzer, K. A.; Fisher, R. A. *J. Am. Chem. Soc.* **1990**, *112*, 4600.

(8) Hidai, M.; Mizobe, Y. *Chem. Rev.* **1995**, *95*, 1115.

(9) Turner, H. W.; Fellmann, J. D.; Rocklage, S. M.; Schrock, R. R.; Churchill, M. R.; Wasserman, H. J. *J. Am. Chem. Soc.* **1980**, *102*, 7809.

(10) Hagadorn, J. R.; Arnold, J. *J. Am. Chem. Soc.* **1996**, *118*, 893.

(11) Duchateau, R.; Gambarotta, S.; Beydoun, N.; Bensimon, C. *J. Am. Chem. Soc.* **1991**, *113*, 8986.

(12) Beydoun, N.; Duchateau, R.; Gambarotta, S. *J. Chem. Soc., Chem. Commun.* **1992**, 244.

Table 5. Bond Lengths (Å) and Angles (deg) for (i-PrNC$_6$H$_4$)(i-PrNC$_6$H$_4$O)Ti(dmpe)

Distances			
Ti−N(2)	1.943(3)	Ti−O(1)	1.961(2)
Ti−N(1)	1.996(2)	Ti−P(l)	2.6238(11)
Ti−C(26)	2.146(4)	Ti−P(2)	2.6138(10)
Ti−C(21)	2.510(3)		

Angles			
N(2)−Ti−O(1)	116.54(11)	N(2)−Ti−N(1)	109.04(11)
O(1)−Ti−N(1)	80.71(10)	N(2)−Ti−C(26)	68.64(14)
O(1)−Ti−C(26)	162.45(12)	N(1)−Ti−C(26)	114.31(12)
N(2)−Ti−P(2)	88.19(8)	O(1)−Ti−P(2)	80.78(7)
N(1)−Ti−P(2)	158.98(8)	C(26)−Ti−P(2)	82.70(9)
O(1)−Ti−P(1)	85.89(7)	N(1)−C(17)−C(19)	111.0(3)
C(26)−Ti−P(1)	84.51(11)	C(11)−O(1)−Ti	114.5(2)
P(2)−Ti−P(1)	76.43(3)	C(16)−N(1)−Ti	111.7(2)
C(16)−N(1)−C(17)	116.3(2)	N(2)−Ti−P(1)	150.64(9)
C(17)−N(1)−Ti	131.6(2)	N(1)−Ti−P(l)	92.37(8)
C(21)−N(2)−Ti	95.9(2)	C(27)−N(2)−Ti	141.2(2)
C(21)−N(2)−C(27)	122.6(3)		

another (O(1)−Ti−C(26) = 162.45(12)°). We propose that the C(26)−O(1) bond is cleaved in intermediate [i-PrNON]Ti(dmpe). The Ti−O bond in (i-PrC$_6$H$_4$)(i-PrC$_6$H$_4$O)Ti(dmpe) (Ti−O(1) = 1.961(2) Å) is shorter than dative Ti−O bonds found in other compounds reported here, consistent with a covalent Ti−O bond. Trans to the oxygen atom is a phenyl group [O(1)−Ti−C(26) = 162.45(12)°] that is part of a strained azatitanabenzocyclobutene ring, a fact that accounts for the acute Ti−C(26)−C(21) angle [86.5(2)°]. The sum of the angles about C(26) and N(2) is ∼360°. The Ti−N and Ti−P distances are in the expected range.

Heating [i-PrNON]Ti(CHCMe$_3$)$_2$ in the presence of excess PMe$_3$ produces the neopentylidene complex [i-PrNON]Ti(CHCMe$_3$)(PMe$_3$)$_2$, which was isolated as green-black crystals in ∼50% yield (eq 10). The ^{1}H and ^{13}C NMR resonances for

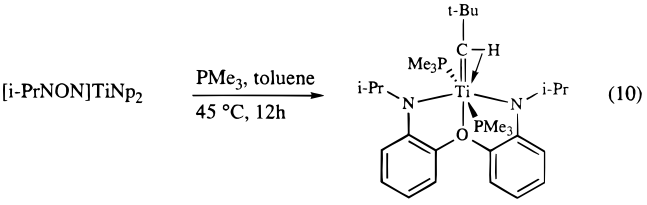

(10)

the neopentylidene H$_\alpha$ and C$_\alpha$ are slightly concentration dependent, consistent with ready dissociation of one PMe$_3$, as found in other pseudooctahedral complexes reported here. The alkylidene proton appears at ∼3 ppm, which is upfield relative to its chemical shift in all other titanium alkylidene complexes ($\delta \approx 12$ ppm),[16] and characteristic of an alkylidene in which there is a significant agostic interaction[17] between the CH$_\alpha$ electron pair and the metal.[18] The gated decoupled ^{13}C NMR spectrum shows a doublet at $\delta \approx 229$ ppm with a low J_{CH} coupling constant (80 Hz). The isopropyl methyl groups are equivalent, which suggests that [i-PrNON]Ti(CHCMe$_3$)(PMe$_3$)$_2$ is C_{2v} symmetric in solution on the NMR time scale. These

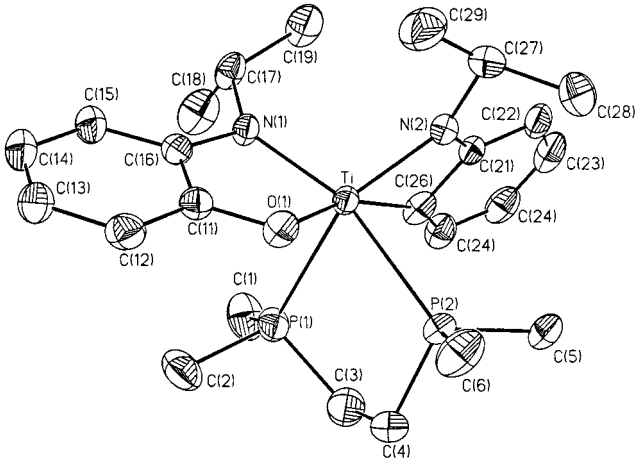

Figure 6. ORTEP diagram (35% probability level) of (i-PrNC$_6$H$_4$)(i-PrNC$_6$H$_4$O)Ti(dmpe).

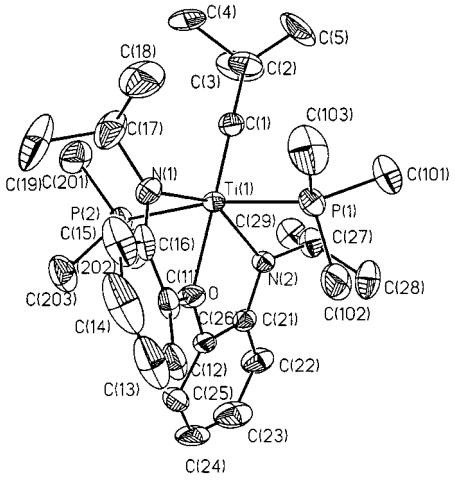

Figure 7. ORTEP diagram (35% probability level) of [i-PrNON]Ti(CHCMe$_3$)(PMe$_3$)$_2$). (Only one orientation of the *tert*-butyl group is shown; see the Experimental Section.)

data are consistent only with a highly distorted neopentylidene ligand in which the α hydrogen is not localized on the NMR time scale. In many neopentylidene complexes, including the first of the high oxidation state type (Ta(CHCMe$_3$)(CH$_2$CMe$_3$)$_3$[18]), the alkylidene H$_\alpha$ is not localized on the NMR time scale, even though the agostic interaction is significant.

An X-ray structure (Tables 1 and 4; Figure 7) revealed that the neopentylidene ligand in [i-PrNON]Ti(CHCMe$_3$)(PMe$_3$)$_2$ is indeed linear [Ti(1)−C(1)−C(2) = 179.3(3)°] with a short Ti−C(1) bond [1.884(4) Å], characteristic of a "distorted" alkylidene in which the CH$_\alpha$ agostic interaction is significant.[18] No electron density could be located in the vicinity of C(1) that could be ascribed to H$_\alpha$. Therefore, we cannot say whether H$_\alpha$ is localized in the solid state or disordered over two or more bonding sites with no detectable disorder in the surrounding ligand set. For comparison, in the only other structurally characterized titanium neopentylidene complex, {Me$_2$PCH$_2$C(O)[o-(CMe$_2$)$_2$C$_6$H$_4$]}CpTi(CHCMe$_3$), a Ti−C bond length of 1.911(3) Å and a Ti−C$_\alpha$−C$_\beta$ bond angle of 158.7(2)° were found.[19] The ligand configuration and Ti−P bond lengths in [i-PrNON]Ti(CHCMe$_3$)(PMe$_3$)$_2$ are similar to those of other species reported here. The *tert*-butyl group was found in two orientations, although the disorder could be solved readily.

(13) de Wolf, J. M.; Blaauw, R.; Meetsma, A.; Teuben, J. H.; Gyepes, R.; Varga, V.; Mach, K.; Veldman, N.; Spek, A. L. *Organometallics* **1996**, *15*, 4977.

(14) Berry, D. H.; Procopio, L. J.; Carroll, P. J. *Organometallics* **1988**, *7*, 570.

(15) Sanner, R. D.; Duggan, D. M.; McKenzie, T. C.; Marsh, R. E.; Bercaw, J. E. *J. Am. Chem. Soc.* **1976**, *98*, 8358.

(16) Beckhaus, R. *Angew. Chem., Int. Ed. Engl.* **1997**, *36*, 687.

(17) Brookhart, M.; Green, M. L. H.; Wong, L. *Prog. Inorg. Chem.* **1988**, *36*, 1.

(18) Schrock, R. R. In *Alkylidene Complexes of the Earlier Transition Metals*; Braterman, P. R., Ed.; Plenum: New York, 1986.

(19) van Doorn, J. A.; van der Heijden, H.; Orpen, A. G. *Organometallics* **1995**, *14*, 1278.

A Study of the Decomposition of [*i*-PrNON]Zr(CH_2CH_3)$_2$. [*i*-PrNON]Zr(CH_2CH_3)$_2$ is the only β-hydrogen-containing dialkyl complex discussed in this paper that decomposes in the absence of PMe_3 cleanly to a single identifiable diamagnetic species. In pentane the product crystallizes out in ~75% yield as small, pale yellow needles that so far have not been suitable for a single-crystal X-ray study. NMR data and combustion analyses are consistent with the product having the composition {[*i*-PrNON]Zr(CH_2CH_3)}$_2$(μ-CH_2CH_2). Since a proton resonance in the same position as that of ethane is observed during decomposition, we propose that the reaction is that shown in eq 11. The isopropyl methyl groups in {[*i*-PrNON]-

$$2[i\text{-PrNON}]ZrEt_2 \xrightarrow[22\ ^\circ C,\ 21\ h,\ -ethane]{pentane} \{[i\text{-PrNON}]ZrEt\}_2(\mu\text{-}C_2H_4) \quad (11)$$

Zr(CH_2CH_3)}$_2$(μ-CH_2CH_2) are diastereotopic, which would be consistent with the expected *mer* configuration of the ligand, but no mirror plane exists that relates the two methyl groups in one isopropyl group. A singlet resonance for the bridging ethylene is found at 1.09 ppm in the ^{1}H NMR spectrum. The μ-ethylene complex decomposes upon heating in solution.

The dimeric formulation of {[*i*-PrNON]Zr(CH_2CH_3)}$_2$(μ-CH_2CH_2) is based upon the characterization of complexes that contain bridging ethylene ligands in the literature. The reported complexes include [$MX_3(PEt_3)_2$]$_2$(μ-η^2:η^2-C_2H_4) (M = Zr, Hf; X = Cl, Br),[20−22] which have type **A** structures,[21,22] and (Cp_2ZrR)$_2$(μ-η^2:η^2-C_2H_4) (R = $ClAlEt_3$,[23] Me[24]) and {[($SiMe_2$)$_2$(η^5-C_5H_3)$_2$]ZrEt}$_2$(μ-η^2:η^2-C_2H_4),[25] which have type **B** structures, perhaps in part as a consequence of greater steric

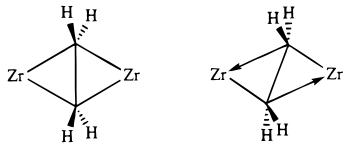

A **B**

crowding in zirconocenes. The J_{CH} coupling constants for the ethylene bridge in (Cp_2ZrMe)$_2$(μ-η^2:η^2-C_2H_4) and {[($SiMe_2$)$_2$-(η^5-C_5H_3)$_2$]ZrEt}$_2$(μ-η^2:η^2-C_2H_4) are 146 and 141 Hz, respectively. The J_{CH} for the "olefinic" ^{13}C resonances in a propylene complex of type **A** were found to be in the range 127−129 Hz.[20] In {[*i*-PrNON]Zr(CH_2CH_3)}$_2$(μ-CH_2CH_2) J_{CH} = 143 Hz. Therefore, on the basis of J_{CH} values, we propose that {[*i*-PrNON]Zr(CH_2CH_3)}$_2$(μ-CH_2CH_2) is of type **B**. It should be noted that {[($SiMe_2$)$_2$(η^5-C_5H_3)$_2$]ZrEt}$_2$(μ-η^2:η^2-C_2H_4) is formed via intermediate [($SiMe_2$)$_2$(η^5-C_5H_3)$_2$]$ZrEt_2$, while (Cp_2-$ZrMe$)$_2$(μ-η^2:η^2-C_2H_4) was obtained upon treatment of [Cp_2-$ZrEt(CH_2{=}CH_2)$]MgBr with [Cp_2ZrMe_2], a reaction that would require transfer of a methyl group from one Zr to the other.

Decomposition of [*i*-PrNON]Zr(CH_2CH_3)$_2$ to {[*i*-PrNON]Zr-(CH_2CH_3)}$_2$(μ-CH_2CH_2) was followed by proton NMR. The decomposition was found to be first order in Zr over a period of more than 2 half-lives for two samples in C_6D_6 at 22 °C with initial concentrations of 0.07 and 0.015 M. The observed rate constants were 0.0078 min^{-1} (R = 0.9998) and 0.0083 min^{-1} (R = 0.9993; Table 6). The observed rate constant for decomposition of [*i*-PrNON]Zr(CH_2CH_3)$_2$ was found to be 0.020 min^{-1} (R = 0.9936; >2 half-lives) at 35 °C. This value should be compared with k_{obs} for decomposition of [*i*-PrNON]Zr-(CD_2CH_3)$_2$ (0.025 min^{-1}; R = 0.9974; >2 half-lives) and [*i*-PrNON]Zr(CD_2CD_3)$_2$ (0.0025 min^{-1}; R = 0.9965; ~1 half-life) at 35 °C. These data suggest that the mechanism of decomposition of [*i*-PrNON]Zr(CH_2CH_3)$_2$ consists of a unimolecular β-hydride abstraction to give ethane and "[*i*-PrNON]-Zr(CH_2CH_2)", which then reacts rapidly with [*i*-PrNON]Zr-(CH_2CH_3)$_2$ to give the observed product (eqs 12 and 13). The

$$[i\text{-PrNON}]ZrEt_2 \xrightarrow{k_1} [i\text{-PrNON}]Zr(CH_2CH_2) + \text{ethane} \quad (12)$$

$$[i\text{-PrNON}]Zr(CH_2CH_2) + [i\text{-PrNON}]ZrEt_2 \xrightarrow{k_2} \{[i\text{-PrNON}]ZrEt\}_2(\mu\text{-}C_2H_4) \quad (13)$$

difference between the rate constant for decomposition of [*i*-PrNON]Zr(CD_2CH_3)$_2$ (0.025 min^{-1}) and that for [*i*-PrNON]-Zr(CH_2CH_3)$_2$ (0.0200 min^{-1}) at 35 °C is evidence for a typically small inverse secondary isotope effect. However, the difference in the observed rate constant for decomposition of [*i*-PrNON]-Zr(CD_2CH_3)$_2$ (0.025 min^{-1}) and [*i*-PrNON]Zr(CD_2CD_3)$_2$ (0.0025 min^{-1}) is clearly indicative of a primary isotope effect of approximately 10 for the β-hydride abstraction step. At 45 °C the decompositions of [*i*-PrNON]Zr(CH_2CH_3)$_2$, [*i*-PrNON]Zr-(CD_2CH_3)$_2$, and [*i*-PrNON]Zr(CD_2CD_3)$_2$ are not as well-behaved as they are at 35 °C, with some curvature in the first-order plot being observed beyond 2 half-lives for [*i*-PrNON]Zr(CH_2CH_3)$_2$ and [*i*-PrNON]Zr(CD_2CH_3)$_2$, and beyond 1 half-life for [*i*-PrNON]-Zr(CD_2CD_3)$_2$. However, the data are useful, if not as accurate, and suggest again an inverse isotope effect of ~0.8 for decomposition of [*i*-PrNON]Zr(CH_2CH_3)$_2$ versus [*i*-PrNON]Zr-(CD_2CH_3)$_2$, and a primary isotope effect of ~7 for decomposition of [*i*-PrNON]Zr(CH_2CH_3)$_2$ versus [*i*-PrNON]Zr(CD_2CD_3)$_2$ at 45 °C (Table 6). The rate constant for the rate-limiting formation of "[*i*-PrNON]Zr(CH_2CH_2)" (k_1; eq 12) would be half the observed rate constant, if the subsequent bimolecular reaction (eq 13) were rapid.

Two plausible ways to form the final product in an intermolecular fashion are β-hydrogen transfer or alkyl transfer (Scheme 1). The product of decomposition of [*i*-PrNON]Zr(CD_2CH_3)$_2$ should be {[*i*-PrNON]Zr(CD_2CH_3)}$_2$(CD_2CH_2) if the alkyl transfer mechanism prevails, whereas intermolecular β-hydrogen abstraction should lead to a 1:1 mixture of {[*i*-PrNON]Zr-

Table 6. A Summary of the Rate Constants for Decomposition of [*i*-PrNON]ZrR_2 Complexes[a]

compound	temp (°C)	rate constant (min^{-1})	R factor
Zr(CH_2CH_3)$_2$	22	0.0078	0.9998
		0.0083	0.9993
	35	0.020	0.9936
	45	0.058	0.9913
Zr(CD_2CH_3)$_2$	35	0.025	0.9974
	45	0.080	0.9865
Zr(CD_2CD_3)$_2$	35	0.0025	0.9965[b]
	45	0.012	0.9978[b]
Zr($CH_2CH_2CH_3$)$_2$	45	0.0036	0.9865[b]
Zr(CH_2CH_3)$_2$/~2.5PMe_3	22	0.052	0.9933[c]
Zr($CH_2CH_2CH_3$)$_2$/~2.5PMe_3	22	0.020	0.9942[d]

[a] Determined by proton NMR following the disappearance of the dialkyl. [b] Followed for approximately 1 half-life. [c] $[Zr]_o$ = 31 mM; $[P]_o$ = 85 mM. [d] $[Zr]_o$ = 33 mM; $[P]_o$ = 85 mM.

(20) Wengrovius, J. H.; Schrock, R. R.; Day, C. S. *Inorg. Chem.* **1981**, *20*, 1844.
(21) Cotton, F. A.; Kibala, P. A. *Polyhedron* **1987**, *6*, 645.
(22) Cotton, F. A.; Kibala, P. A. *Inorg. Chem.* **1990**, *29*, 3192.
(23) Kaminsky, W.; Kopf, J.; Sinn, H.; Vollmer, H.-J. *Angew. Chem., Int. Ed. Engl.* **1976**, *15*, 629.
(24) Takahashi, R.; Kasai, K.; Suzuki, N.; Nakajima, K.; Negishi, E. *Organometallics* **1994**, *13*, 3413.
(25) Fernandez, F. J.; Gomez-Sal, P.; Manzanero, A.; Royo, P.; Jacobsen, H.; Berke, H. *Organometallics* **1997**, *16*, 1553.

Scheme 1

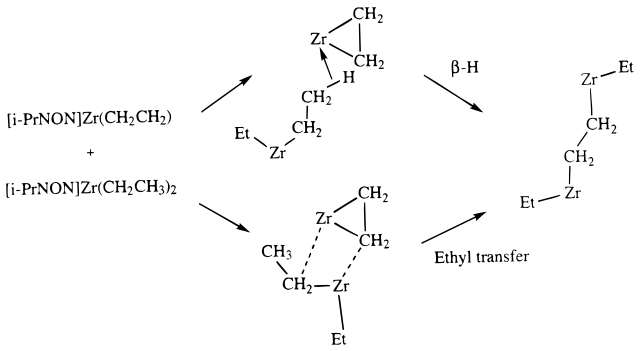

$(CD_2CH_3)\}_2(CD_2CH_2)$ and $[i\text{-PrNON}]_2Zr_2(CH_2CD_2H)(CD_2CH_3)$-$(CD_2CH_2)$, assuming no isotope effect of any kind *and an equal probability of adding a proton to each end of the ethylene* in intermediate $[i\text{-PrNON}]Zr(CD_2CH_2)$. In the latter case the ratio of D attached to C_α of an ethyl group, C_β of an ethyl group, and an ethylene carbon should be 3:1:2; i.e., ~17% of the deuterium should be in the β position of an ethyl group. This labeling study was carried out, and by ^2H NMR no deuterium could be detected in the β position of an ethyl group. Therefore, these data suggest either that an alkyl group transfers from one Zr to the other in the second (fast) step of the reaction *or* that the H_β in an ethyl group on one zirconium transfers virtually exclusively to the CH_2 end of the η^2-CH_2CD_2 ligand in the intermediate.

A ^{13}C labeling study also was undertaken to eliminate any possibility of a dramatic isotope effect altering the reaction pathway. $[i\text{-PrNON}]Zr(^{13}CH_2CH_3)_2$ was prepared by treating $[i\text{-PrNON}]ZrCl_2$ with $CH_3{}^{13}CH_2MgI$, and its decomposition in C_6D_6 was followed by ^{13}C NMR at 22 °C. The reaction was allowed to proceed 2/3 of the way to completion, i.e., until the ratio of $[i\text{-PrNON}]ZrEt_2$ to $\{[i\text{-PrNON}]ZrEt\}_2(\mu\text{-}C_2H_4\}$ was 1:1. In the ^{13}C NMR spectrum of this mixture the weak intensity of the resonance for $ZrCH_2{}^{13}CH_3$ in $\{[i\text{-PrNON}]ZrEt\}_2(\mu\text{-}C_2H_4\}$ was entirely consistent with naturally abundant ^{13}C; i.e., there is no evidence for the ^{13}C-labeled carbon being in the β position of an ethyl group in the product. These results are again consistent either with transfer of an ethyl group from $ZrEt_2$ to the $Zr(\eta^2\text{-}C_2H_4)$ intermediate or with proton transfer selectively to a ^{12}C carbon atom in the $Zr(\eta^2\text{-}C_2H_4)$ intermediate that has no time or opportunity to equilibrate with the ^{13}C-labeled end of the ethylene fragment. We favor the ethyl transfer proposal (eq 14), since there is precedent in the literature for a methyl transfer in zirconocene systems to give an analogous μ-CH_2CH_2 complex.[24]

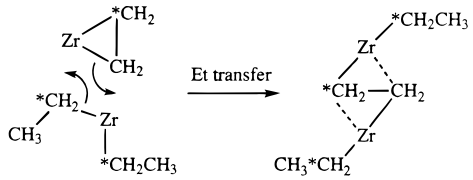

(14)

Decomposition of $[i\text{-PrNON}]ZrPr_2$ does not yield any characterizable product, e.g., an analogous bridging propylene complex, although such species have been observed in other systems.[20] At 45 °C $[i\text{-PrNON}]ZrPr_2$ decomposes in a first-order manner in C_6D_6 at a rate that is approximately 16 times slower than the rate at which $[i\text{-PrNON}]ZrEt_2$ decomposes (Table 6). Since the mechanism of decomposition of $[i\text{-PrNON}]ZrPr_2$ may not be analogous to that of $[i\text{-PrNON}]ZrEt_2$, the relative rates of β abstraction in the two species are uncertain. The significantly slower rate of decomposition of $[i\text{-PrNON}]ZrPr_2$ is at least consistent with what has been observed in zirconocene systems, namely, the greater stability of zirconocene dipropyl intermediates compared to zirconocene diethyl intermediates.[5]

The rate of decomposition of $[i\text{-PrNON}]ZrEt_2$ at 22 °C in C_6D_6 in the presence of ~2.5 equiv of PMe_3 is also first order in Zr through >2 half-lives ($k_{obs} = 0.052$ min^{-1}), which is much faster than decomposition of $[i\text{-PrNON}]ZrEt_2$ in the absence of PMe_3 ($k_{obs} = 0.0078$ min^{-1}, Table 6). Under the same conditions the observed rate constant for decomposition of $[i\text{-PrNON}]ZrPr_2$ is 0.020 min^{-1}. We conclude that the decomposition of the dialkyl complexes is induced by phosphine. On the basis of the structure of isolated $[i\text{-PrNON}]Zr(CH_2CHMe_2)_2(PMe_3)$, we propose that $[i\text{-PrNON}]ZrR_2$ and PMe_3 are in equilibrium with $[i\text{-PrNON}]ZrR_2(PMe_3)$, and that the equilibrium constant is large enough that a first-order decay in zirconium is observed even as phosphine is consumed to form the product. The equilibrium constant for formation of an adduct in which the alkyls are smaller than isobutyl (Et and Pr) should be even larger than it is in isolated $[i\text{-PrNON}]Zr(CH_2CHMe_2)_2(PMe_3)$. It should be noted that one phosphine is labile in the observed olefin products, so the concentration of phosphine actually may change by a factor of only 2−3 under the stated conditions. A full treatment of the decomposition to establish the true rate constant for decomposition of $[i\text{-PrNON}]ZrR_2(PMe_3)$, as well as equilibrium constants for formation of the monophosphine adducts, is beyond the scope of this paper.

Synthesis of Titanium and Zirconium Complexes That Contain $[CyNON]^{2-}$. Condensation between cyclohexanone and $O(o\text{-}C_6H_4NH_2)_2$ in acetic acid in the presence of excess zinc at 65 °C cleanly afforded $H_2[CyNON]$ in ~90% yield (eq 15). $H_2[CyNON]$ is an air-stable, yellow viscous oil that is soluble in common solvents; it occasionally crystallizes at room temperature after several weeks.

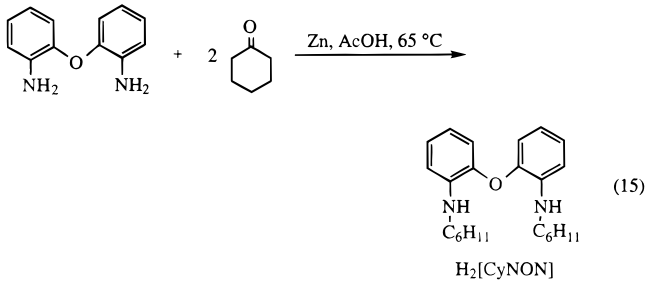

(15)

The syntheses of $[CyNON]ZrCl_2$ (eq 16) and $[CyNON]TiCl_2$ (eq 17) are entirely analogous to those for $[i\text{-PrNON}]MCl_2$. The

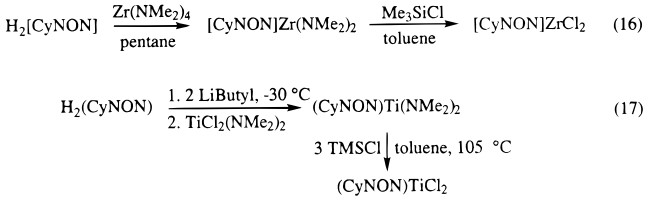

(16)

(17)

dichloride complexes react with lithium reagents in toluene or magnesium reagents in diethyl ether to give the dialkyl complexes $[CyNON]MR_2$ (M = Zr, R = Me, Et, *i*-Bu, CH_2CMe_3, allyl; M = Ti, R = Me, CH_2CMe_3, *i*-Bu) in moderate to excellent yields. Proton and carbon NMR spectra of the dialkyl complexes are all consistent with a structure that has C_2 or C_{2v} symmetry. We presume that they are all *mer* structures by analogy with crystallographically characterized $[i\text{-PrNON}]^{2-}$ structures discussed above. The reaction between $H_2[CyNON]$

and $Zr(CH_2SiMe_3)_4$ in toluene or benzene at room temperature gave $[CyNON]Zr(CH_2SiMe_3)_2$ in high yield. In contrast, attempts to react $H_2[CyNON]$ with $Zr(CH_2Ph)_4$ or $Zr(CH_2CMe_3)_4$ (70 °C for 3.5 days and 70 °C for 7 days, respectively) did not yield the expected dialkyl complexes; no products could be identified.

The dimethyl, dineopentyl, and bis(trimethylsilylmethyl) complexes are stable in solution at room temperature for days, according to their proton NMR spectra. For example, a toluene-d_8 solution of $[CyNON]Zr(CH_2SiMe_3)_2$ (~0.16 M) showed <5% decomposition after being heated to 100 °C for 3 days. In contrast, orange $[CyNON]Ti(i\text{-}Bu)_2$ (~8 mM in C_6D_6) decomposed at room temperature over a period of several hours. Solutions of $[CyNON]Zr(i\text{-}Bu)_2$ (~7 mM in C_6D_6) show no signs of decomposition at room temperature after 24 h, but solutions decompose readily at 100 °C with an accompanying rapid color change from colorless to deep red. $[CyNON]ZrEt_2$ decomposes over a period of 1 h at room temperature.

Decomposition of $[CyNON]ZrEt_2$ in neat trimethylphosphine yielded orange $[CyNON]Zr(\eta^2\text{-}C_2H_4)(PMe_3)_2$ in ~70% isolated yield (eq 18), while a similar reaction between $[CyNON]Zr(i\text{-}Bu)_2$ and neat PMe_3 requires a temperature of 50 °C over a period of 3 days in the dark to yield $[CyNON]Zr(H_2C{=}CMe_2)(PMe_3)_2$.

$$(CyNON)ZrR_2 \xrightarrow{\text{excess } PMe_3} (CyNON)Zr(\eta^2\text{-}C_2H_2R'_2)(PMe_3)_2 \quad \begin{matrix} R = Et,\ i\text{-}Bu \\ R' = H,\ Me \end{matrix} \tag{18}$$

All of the $[CyNON]^{2-}$ chemistry that we have explored appears to be entirely analogous to the $[i\text{-}PrNON]^{2-}$ chemistry. Evidently the increased steric bulk of the cyclohexyl group compared to the isopropyl group is of no consequence, as one might have surmised on the basis of the X-ray structures of the $[i\text{-}PrNON]^{2-}$ complexes reported here. Since the $[CyNON]^{2-}$ chemistry is so similar to the $[i\text{-}PrNON]^{2-}$ chemistry, the experimental details of the synthesis of metal complexes are provided as Supporting Information.

Generation of Cations and Their Reactions with 1-Hexene. The reaction between $[CyNON]ZrMe_2$ and $[HNMe_2Ph][B(C_6F_5)_4]$ in bromobenzene-d_5 at −35 °C led to a single species whose ^1H NMR spectrum at 0 °C exhibited a singlet at 0.65 ppm of area 3, consistent with the formation of a cationic complex $\{[CyNON]ZrMe(NMe_2Ph)\}^+$. $\{[CyNON]ZrMe(NMe_2Ph)\}^+$ appears to be stable in solution at temperatures below 10 °C, but decomposes slowly at room temperature, according to ^1H NMR spectra.

Addition of 50 equiv of 1-hexene to a bromobenzene-d_5 solution of $\{[CyNON]ZrMe(NMe_2Ph)\}[B(C_6F_5)_4]$, generated as above at ~0 °C, led to slow oligomerization of 1-hexene. New olefinic resonances were observed in the range 5.42−5.34 ppm, a region that is consistent with them being internal olefinic protons, e.g., the product of β elimination from a 2,1 insertion product.[26] The intensity suggests that approximately 10 equiv of 1-hexene was consumed for every two olefinic protons in an end group. Analogous reactions involving $[i\text{-}PrNON]ZrMe_2$ activated by $[Ph_3C][B(C_6F_5)_4]$ in bromobenzene-d_5 at 0 °C produced similar results.

These data suggest that activated $[CyNON]^{2-}$ or $[i\text{-}PrNON]^{2-}$ complexes of the type described here are not successful polymerization catalysts. Further studies will be necessary to assess exactly what oligomeric products are formed in such circumstances, and by what mechanism, and whether oligomerization of some monomers (e.g., ethylene) might produce oligomers with a molecular weight in an unusual range. The main point is that the difference in behavior between cationic $[i\text{-}PrNON]^{2-}$ initiators and $[t\text{-}BuNON]^{2-}$ initiators[1−3] for the polymerization of 1-hexene is dramatic.

Discussion

The results reported here suggest that complexes that contain the $[i\text{-}PrNON]^{2-}$ ligand are significantly less crowded than those that contain the $[t\text{-}BuNON]^{2-}$ ligand, and that dialkyl complexes that contain the $[t\text{-}BuNON]^{2-}$ ligand[3] are less stable than $[i\text{-}PrNON]^{2-}$ complexes, especially for titanium. For example, $[i\text{-}PrNON]Ti(CH_2CHMe_2)_2$ and $[i\text{-}PrNON]Ti(CH_2CMe_3)_2$ can both be prepared, while only $[t\text{-}BuNON]TiMe_2$ could be prepared. While the *tert*-butyl group is a slightly better electron donor than an isopropyl group, that difference alone would not appear to be significant enough to produce a dramatically lower stability for $[t\text{-}BuNON]TiR_2$ complexes. It should be noted, however, that the greater instability of $[t\text{-}BuNON]TiR_2$ complexes cannot be ascribed automatically to decomposition processes that involve β-hydrogen abstraction or homolytic Ti−C bond cleavage; alternatives such as N−*t*-Bu bond cleavage cannot be eliminated.

It also seems clear now that the *mer* structure (twisted) is the lowest energy structure for $[i\text{-}PrNON]MR_2$ structures, at least those whose structures we have determined, and that the (twisted) *fac* structures found for $[t\text{-}BuNON]MR_2$ complexes can be ascribed to steric crowding between the *tert*-butyl group and the MR_2 groups. Although most metal−ligand bond distances are not dramatically different in the two species, there is some tendency for $M-O_{donor}$ bonds to be shorter in *mer* complexes, perhaps as a consequence of some M−O π bonding, which is possible only in *mer* species. In *mer*-$[i\text{-}PrNON]ZrMe_2$ the isopropyl hydrogen atoms point directly between the methyl groups, while the isopropyl methyl groups are located on each side of the phenylene ring. The ligand backbone is still twisted to some extent as a consequence of an interaction between the two aryl protons next to the oxygen donor. If $[t\text{-}BuNON]ZrMe_2$ were to adopt the same *mer* structure as $[i\text{-}PrNON]ZrMe_2$, the additional methyl group in each amido substituent would point between the two zirconium methyl groups. To minimize that steric interaction, the ligand therefore twists further into the *fac* form.

The issues concerning a *mer* versus a *fac* structure have been in the literature for some time for similar dianionic/donor ligands bound to a main group element such as tin.[27] For example, Holmes[28] has reported the structures of the cyclic stannanes $(t\text{-}Bu)_2Sn[(OCH_2CH_2)_2NMe]$, a *mer* structure, and $Me_2Sn[(SCH_2CH_2)_2NMe]$, a *fac* structure with a relatively long Sn−S bond. NMR data[29−31] support interconversion of *mer* and *fac* structures, and actual dissociation of the amine donor at higher temperatures, especially in the sulfur case. In rare cases both *mer* and *fac* isomers have been observed in solution. However, steric factors would not play the same role in these systems as in the systems reported here.

(26) Resconi, L.; Piemontesi, F.; Camurati, I.; Sudmeijer, O.; Nifant'ev, I. E.; Ivchenko, P. V.; Kuz'mina, L. G. *J. Am. Chem. Soc.* **1998**, *120*, 2308.

(27) Holmes, R. R. *Prog. Inorg. Chem.* **1984**, *32*, 119.

(28) Swisher, R. G.; Holmes, R. R. *Organometallics* **1984**, *3*, 365.

(29) Zschunke, A.; Tzschach, A.; Jurkschat, K. *J. Organomet. Chem.* **1976**, *112*, 273.

(30) Jurkschat, K.; Mügge, C.; Tzschach, A.; Zschunke, A.; Larin, M. F.; Pestunovich, V. A.; Voronkov, M. G. *J. Organomet. Chem.* **1977**, *139*, 279.

(31) Mügge, C.; Jurkschat, K.; Tzschach, A.; Zschunke, A. *J. Organomet. Chem.* **1979**, *164*, 135.

The [*i*-PrNON]MR_2 and [CyNON]MR_2 complexes are much more stable than analogous Cp_2MR_2 complexes, especially when M = Ti. For example, $Cp_2Ti(CH_2CMe_3)_2$ can be isolated only below 0 °C.[32] Also, it is known that Cp_2TiEt_2, prepared in situ from Cp_2TiCl_2 and EtMgCl, cleanly decomposes in the presence of PMe_3 to yield $Cp_2Ti(PMe_3)_2$.[33] Cp_2ZrEt_2 is also not isolable, although Cp_2HfEt_2 is isolable, consistent with a greater stability toward β-hydride elimination in the order R = Et < *n*-Pr < *i*-Bu,[5,6] at least for zirconocene complexes of the type Cp_2ZrR_2. (For a more extensive discussion of group 4 metal dialkyl complexes, especially of nitrogen-based ligands, see a related paper concerning [*t*-BuNON]$^{2-}$ complexes.[3])

Dialkyl metallocenes appear to be inherently more crowded than the dialkyl complexes discussed here, which could help explain the generally wider C−M−C angles in the complexes reported here compared to, for example, the C−Zr−C angle in Cp_2ZrMe_2 (95.6(12)°[34]). Therefore, when a donor adds to a Cp_2ZrR_2 complex, it generally does so *between* the two alkyl groups. In contrast, in [*i*-PrNON]$Zr(CH_2CHMe_2)_2$ a phosphine can more readily approach the metal from outside the C−Zr−C wedge, a process that consequently pushes the alkyl groups toward one another. Therefore, phosphines do not accelerate β-hydrogen abstraction in Cp_2MR_2 complexes,[5,6] in contrast to the accelerated β-hydrogen abstraction in [*i*-PrNON]MR_2 complexes found here. In Cp_2ZrH_2 a central coordination of PMe_3 to zirconium has been observed.[35] In short the orbital between the two alkyl groups in a d^0 metallocene is believed to be the most Lewis acidic one,[36] as well as the one that is sterically most accessible. There are exceptions, e.g., the reaction of CO with zirconocene dialkyl and diaryl complexes. Low-temperature NMR and IR studies by Erker showed that initially CO inserts into one of the two zirconium carbon bonds to give a lateral η^2-acetyl complex that rearranges at higher temperature to the thermodynamically more stable central product.[37,38]

The formation of stable alkylidene complexes of group 4 metals by α-hydrogen abstraction is rare, although more examples are known for titanium[16] than for zirconium.[39] It is interesting to note that if only one π bond between Ti and the amido nitrogens is invoked (involving the unsymmetric combination of p orbitals on amido nitrogens), then six orbitals are involved in binding the [*i*-PrNON]$^{2-}$ ligand and two phosphines to the metal, leaving two π orbitals (e.g., d_{xz} and d_{yz}) and a σ orbital (e.g., d_{z^2}) for binding to the neopentylidene ligand. In the presence of d_{xz} and d_{yz} orbitals that are close in energy and an approximately 4-fold symmetric sterically demanding coordination pocket, the neopentylidene ligand adopts a near linear configuration with apparently little energy difference between an agostic C−H_α interaction along the N−Ti−N axis or along the P−Ti−P axis. It seems surprising that the energy difference between the two d orbitals of π type symmetry would be so small. Therefore, steric interactions between the *tert*-butyl group and the isopropyl or phosphine methyl groups may be a significant factor in generating and stabilizing a linear neopentylidene ligand with a significant agostic interaction. Similar arguments were put forth to explain the formation of essentially linear alkylidenes with significant agostic interactions in $[(Me_3SiNCH_2CH_2)_3N]Ta(CHR)$ complexes,[40] in which the coordination pocket is 3-fold symmetric.

Reports of cleavage of an aryl−oxygen bond are rare in the organometallic literature. Milstein and co-workers[41] have documented C−O cleavage of alkyl− and aryl−oxygen bonds by Rh(I), Pd(II), and Ni(II), while Dehnicke and co-workers have observed activation of a C−O bond in THF by what is believed to be a Ti(II) intermediate,[42] similar to what we propose in this paper. We were surprised by cleavage of the aryl−oxygen bond in the presence of isopropyl amido substituents, which at one time we presumed would be susceptible to CH bond activation at carbon either α or β to the amido nitrogen. Zirconium complexes that contain the $[(i\text{-PrNC}_6H_4)_2S]^{2-}$ or $[(t\text{-BuNC}_6H_4)_2S]^{2-}$ ligands also have been prepared recently, but only $[(i\text{-PrNC}_6H_4)_2S]ZrR_2$ complexes were stable, $[(i\text{-PrNC}_6H_4)_2S]Zr(CH_2CHMe_2)_2$ even at elevated temperatures (80 °C). The reason for the thermal instability of $[(t\text{-BuNC}_6H_4)_2S]ZrMe_2$ could not be determined; C−S bond cleavage must now be considered, along with loss of a *tert*-butyl group.[43]

Zirconium olefin complexes of the type $Cp_2Zr(\eta^2\text{-}CH_2CHR)(PMe_3)$ (R = H, Me, Et) have been known for some time.[33,44,45] Nevertheless, [*i*-PrNON]$Zr(\eta^2\text{-}CH_2CHMe_2)(PMe_3)_2$ appears to be the first example of a stable zirconium complex bearing a 1,1-disubstituted olefin. The first group 4 isobutylene complex $Cp_2Hf(\eta^2\text{-}CH_2CMe_2)(PMe_3)$ was reported by Buchwald and co-workers.[7] In the zirconium system, activation of the Cp ligand was observed.

A limited number of titanium dinitrogen complexes have been reported that contain nitrogen-based ligands, i.e., $\{[PhC(NTMS)_2]_2Ti\}_2(\mu\text{-}N_2)$[10] (Ti−($\mu$-$N_2$) = 1.771(5), 1.759(5) Å; N−N = 1.275(6) Å), $[(TMS_2N)TiCl(tmeda)]_2(\mu\text{-}N_2)$[11] (Ti−($\mu$-$N_2$) = 1.762(5) Å; N−N = 1.289(9) Å), and $[(TMS_2N)TiCl(pyridine)_2]_2(\mu\text{-}N_2)$[12] (Ti−($\mu$-$N_2$) = 1.759(3) Å; N−N = 1.263(7) Å). The N−N bond lengths suggest that the dinitrogen is more reduced in these complexes than in metallocene systems, consistent with a greater reducing ability of a Ti(II) metal center supported by nitrogen-based ancillary ligands. As noted above, complexes that contain the [*i*-PrNON]$M(PMe_3)_2$ core appear to be poised to form two strong orthogonal π bonds, much as complexes that contain a triamidoamine ligand system,[46] and are strongly reducing. Therefore, formation of a μ-dinitrogen complex is perhaps not surprising. However, we were somewhat surprised that dinitrogen binding to "[*i*-PrNON]$Ti(PMe_3)_2$" competes with aryl C−O bond cleavage.

One of the main goals of this research was to attempt to determine the extent to which the *tert*-butyl groups create a coordination sphere in "$\{[t\text{-BuNON}]ZrR\}^+$" that leads to a living polymerization of 1-hexene. Although this aspect of the study is not finished, it is clear that "$\{[i\text{-PrNON}]ZrR\}^+$" will only oligomerize 1-hexene, we presume at this stage because of more

(32) van der Heijden, H.; Hessen, B. *J. Chem. Soc., Chem. Commun.* **1995**, 145.
(33) Binger, P.; Müller, P.; Benn, R.; Rufinska, A.; Gabor, B.; Krüger, C.; Betz, P. *Chem. Ber.* **1989**, *122*, 1035.
(34) Hunter, W. E.; Hrncir, D. C.; Vann Bynum, R.; Penttila, R. A.; Atwood, J. L. *Organometallics* **1983**, *2*, 750.
(35) Lee, H.; Desrosiers, P. J.; Guzei, I.; Rheingold, A. L.; Parkin, G. *J. Am. Chem. Soc.* **1998**, *120*, 3255.
(36) Crabtree, R. H. *The Organometallic Chemistry of the Transition Metals*, 2nd ed.; John Wiley & Sons: New York, 1994; p 121.
(37) Erker, G.; Rosenfeldt, F. *Angew. Chem., Int. Ed. Engl.* **1978**, *17*, 605.
(38) Erker, G.; Rosenfeldt, F. *J. Organomet. Chem.* **1980**, *188*, C1.
(39) Fryzuk, M. D.; Mao, S. S. H.; Zaworotko, M. J.; MacGillivray, L. R. *J. Am. Chem. Soc.* **1993**, *115*, 5336.
(40) Freundlich, J. S.; Schrock, R. R.; Davis, W. M. *J. Am. Chem. Soc.* **1996**, *118*, 3643.
(41) van der Boom, M. E.; Liou, S.-Y.; Ben-David, Y.; Shimon, L. J. W.; Milstein, D. *J. Am. Chem. Soc.* **1998**, *120*, 6531.
(42) Mommertz, A.; Leo, R.; Massa, W.; Harms, K.; Dehnicke, K. *Z. Anorg. Allg. Chem.* **1998**, *624*, 1647.
(43) Schrock, R. R.; Seidel, S. W.; Schrodi, Y.; Davis, W. M. *Organometallics* **1999**, *118*, 428−437.
(44) Alt, H. G.; Denner, C. E.; Thewalt, U.; Rausch, M. D. *J. Organomet. Chem.* **1988**, *356*, C83.
(45) Buchwald, S. L.; Watson, B. T.; Huffman, J. C. *J. Am. Chem. Soc.* **1987**, *109*, 2544.
(46) Schrock, R. R. *Acc. Chem. Res.* **1997**, *30*, 9.

facile β elimination. We hypothesize that the more crowded coordination sphere in "{[*t*-BuNON]ZrR}$^+$" encourages 1,2-insertion and slows β-hydride elimination. In contrast, the much more open coordination sphere of "{[*i*-PrNON]ZrR}$^+$" allows for a significant degree of 2,1 insertion to give a less reactive insertion product that consequently builds up during an oligomerization or polymerization reaction, and that is also likely to be much less stable toward β elimination. Therefore, only oligomers are formed. This proposal is analogous to that put forth recently to account for the oligomerization or polymerization of propylene to give relatively low molecular weight polymers under a variety of circumstances.[47−51]

In future studies we hope to outline further the importance of steric factors in directing insertion reactions in cationic diamido/donor Zr or Hf metal complexes, and in correlating the efficacy of polymerization with steric hindrance, the nature of the donor, and the nature of the connecting link between the donor and the amido ligand. Diamido/donor complexes of the type that have yielded observable, if not always well-behaved, cationic complexes of zirconium or hafnium utterly fail to yield stable Ti cations. The reasons are not known at this time.

Experimental Section

General Procedures. Unless otherwise noted all manipulations were performed under rigorous exclusion of oxygen and moisture in a dinitrogen-filled glovebox or using standard Schlenk procedures. Ether, THF, and pentane were sparged with dinitrogen followed by passage through two 1 gal columns of activated alumina. Toluene and benzene were distilled from benzophenone ketyl. ^{31}P spectra are referenced versus an external standard of 85% H_3PO_4 ($\delta = 0$). All NMR spectra are recorded at room temperature in C_6D_6 unless otherwise noted. Temperatures during variable-temperature NMR studies were not calibrated. Assignments of aromatic ligand resonances in ^{1}H and ^{13}C spectra are not given. Coupling constants are usually not given.

$TiCl_2(NMe_2)_2$,[52] $(2\text{-}NO_2C_6H_4)_2O$,[53] $(2\text{-}NH_2C_6H_4)_2O$,[54] and Me_3CCH_2MgCl[55] were prepared according to literature procedures. 2,4-Dimethyl-6-nitrophenol[56] was prepared according to a procedure reported for 2-*tert*-butyl-4-methylnitrophenol.[57] PMe_3, DMPE (Strem Chemicals), and 1,4-dioxane (anhydrous, Aldrich) were stored under dinitrogen over 4 Å molecular sieves. All other reagents were used as received. Zinc dust (97.5%) was purchased from Strem Chemicals and activated with 5% aqueous HCl prior to use.[4] C_6D_6 and toluene-d_8 (Cambridge Isotope Laboratories) were degassed with dinitrogen and dried over 4 Å molecular sieves for ~1 day prior to use. NMR spectra were recorded in C_6D_6 at 22 °C, unless otherwise noted. $CDCl_3$ (Cambridge Isotope Laboratories) was used as received. Elemental analyses were performed in our laboratories on a Perkin-Elmer 2400 CHN analyzer or by H. Kolbe, Mikroanalytisches Laboratorium (Mühlheim an der Ruhr, Germany).

All kinetic studies were carried out by proton NMR techniques at either 300 or 500 MHz in C_6D_6. Temperatures did not change more than 0.1 °C. Sublimed ferrocene was used as an internal standard (δ = 4.01). The resonance for the NC*H*Me_2 proton of the starting material was monitored in all cases, since it does not overlap with resonances of other products or byproducts.

(*i*-PrNHC$_6$H$_4$)$_2$O (H$_2$[*i*-PrNON]). A 250 mL one-neck flask was charged with $(2\text{-}NH_2C_6H_4)_2O$ (10.0 g, 50 mmol), acetone (15 mL), activated Zn dust (25.0 g, 382 mmol), and glacial acetic acid (100 mL). The flask was capped with a rubber septum, connected to an oil-bubbler via a needle, and then heated under rapid stirring to 60 °C for 24 h. The reaction mixture was poured onto a mixture of ice (200 mL), concentrated aqueous NH_3 (200 mL), and methylene chloride (150 mL). The layers were separated, and the aqueous layer was extracted with methylene chloride (2 × 100 mL). The combined methylene chloride layers were dried over $MgSO_4$. Removal of the methylene chloride in vacuo afforded an orange oil. The oil was dissolved in acetone (150 mL), and concentrated HCl (10 mL) was added. Within 1 min colorless crystals began to form. The mixture was allowed to stand overnight, and the colorless crystalline solid was then filtered off, washed with acetone, and dried. A mixture of aqueous NaOH (100 mL, 10%) and ether (100 mL) was added to this solid. The mixture was stirred until the solid had dissolved. The layers were separated, and the aqueous layer was extracted with ether (3 × 50 mL). The combined organic layers were dried over $MgSO_4$. Activated charcoal was added prior to the layers being filtered through a bed of Celite. Ether was removed in vacuo, leaving a pale yellow oil, yield 13.2 g (93%). The product slowly darkens in air and is therefore best stored under dinitrogen: ^{1}H NMR δ 6.98 (t, 2), 6.88 (d, 2), 6.63 (d, 2), 6.55 (t, 2), 4.14 (br s, 2, N*H*), 3.37 (br m, 2, C*H*Me_2), 0.89 (d, 12, CH*Me*$_2$); ^{13}C NMR δ 144.8, 140.0, 125.1, 118.8, 117.1, 112.5, 44.4 (*C*HMe$_2$), 23.2 (CH*Me*$_2$); HRMS (EI) calcd for $C_{18}H_{24}N_2O$ 284.18886, found 284.18875. Anal. Calcd for $C_{18}H_{24}N_2O$: C, 76.02; H, 8.51; N, 9.85. Found: C, 76.13; H, 8.39; N, 9.81.

[*i*-PrNON]TiCl$_2$. A solution of LiBu in hexane (34 mL, 2.6 M) was added to a solution of H$_2$[*i*-PrNON] (12.48 g, 43.9 mmol) in ether (250 mL) at −25 °C. The solution was allowed to warm to room temperature and was stirred for 10 h. The solution was then cooled to −25 °C, and $TiCl_2(NMe_2)_2$ (9.10 g, 44.0 mmol) was added. The mixture was allowed to warm to room temperature and stirred for 9 h. All volatile components were removed in vacuo, and the residue was extracted with pentane (250 mL) for 15 min. An off-white solid was filtered off and the pentane removed in vacuo. Proton and carbon NMR spectra of the residue, a dark orange oil, were consistent with it being (*i*-PrNON)Ti(NMe$_2$)$_2$: ^{1}H NMR δ 7.30 (d, 2), 7.00 (t, 2), 6.80 (d, 2), 6.48 (t, 2), 4.29 (sept, 2, C*H*Me_2), 3.07 (s, 12, N*Me*$_2$), 1.40 (d, 12, CH*Me*$_2$); ^{13}C NMR δ 148.5, 146.3, 125.5, 115.2, 114.8, 114.0, 54.7 (*C*HMe$_2$), 46.8 (N*Me*$_2$), 23.7 (CH*Me*$_2$).

Toluene (150 mL) and Me_3SiCl (30 g, 276 mmol) were added to the (*i*-PrNON)Ti(NMe$_2$)$_2$ obtained above. This mixture was heated to 110 °C in a sealed heavy-wall 500 mL one-neck flask behind a blast shield. During the reaction the color changed from orange to deep purple-black. After 21 h the solution was allowed to cool to room temperature. The reaction flask was then brought into a drybox and stored at −25 °C overnight to complete formation of black crystals. The supernatant was decanted off, and the black needles were washed liberally with pentane and dried in vacuo: yield 14.70 g (83%); ^{1}H NMR δ 7.09 (d, 2), 6.72 (t, 2), 6.42 (m, 4), 5.91 (sept, 2, C*H*Me_2), 1.45 (d, 12, CH*Me*$_2$); ^{13}C NMR δ 150.6, 145.0, 125.5, 119.7, 114.3, 111.4, 54.6 (*C*HMe$_2$), 18.6 (CH*Me*$_2$). Anal. Calcd for $C_{18}H_{22}Cl_2N_2OTi$: C, 53.89; H, 5.53; N, 6.98. Found: C, 53.95; H, 5.59; N, 6.94.

[*i*-PrNON]TiMe$_2$. A solution of MeMgI in ether (420 μL, 3.0 M) was added to a suspension of [*i*-PrNON]$TiCl_2$ (250 mg, 623 μmol) in toluene (10 mL) at −25 °C. The solution was allowed to warm to room temperature and stirred for 2 h. Dioxane (135 mg, 1.53 mmol) was added, and the solution was filtered through Celite. The filtrate was concentrated to ~1 mL, layered with pentane (2 mL), and stored at −25 °C overnight. Orange microcrystals formed: yield 129 mg (57%); ^{1}H NMR δ 7.36 (d, 2), 6.91 (t, 2), 6.83 (d, 2), 6.45 (t, 2), 5.97 (sept, 2, C*H*Me_2), 1.61 (d, 12, CH*Me*$_2$), 0.94 (s, 6, Ti*Me*$_2$); ^{13}C NMR δ 148.8, 145.3, 125.1, 116.2, 113.6, 112.1, 56.8 (Ti*Me*$_2$), 49.5 (*C*HMe$_2$), 19.6 (CH*Me*$_2$). Anal. Calcd for $C_{20}H_{28}N_2OTi$: C, 66.67; H, 7.83; N, 7.77. Found: C, 66.52; H, 7.85; N, 7.64.

(47) Resconi, L.; Piemontesi, F.; Balboni, D.; Sironi, A.; Moret, M.; Rychlicki, H.; Zeigler, R. *Organometallics* **1996**, *15*, 5046.
(48) Busico, V.; Cipullo, R.; Chadwick, J. C.; Modder, J. F.; Sudmeijer, O. *Macromolecules* **1994**, *27*, 7538.
(49) Busico, V.; Cipullo, R.; Talarico, G.; Segre, A. L.; Caporaso, L. *Macromolecules* **1998**, *31*, 8720.
(50) Busico, V.; Cipullo, R.; Talarico, G. *Macromolecules* **1998**, *31*, 2387.
(51) Guerra, G.; Longo, P.; Cavallo, L.; Corradini, P.; Resconi, L. *J. Am. Chem. Soc.* **1997**, *119*, 4394.
(52) Benzing, E.; Kornicker, W. *Chem. Ber.* **1961**, *94*, 2263.
(53) Wilshire, J. F. K. *Aust. J. Chem.* **1988**, *41*, 995.
(54) Randall, J. J.; Lewis, C. E.; Slagan, P. M. *J. Org. Chem.* **1962**, *27*, 4098.
(55) Schrock, R. R.; Sancho, J.; Pederson, S. F. *Inorg. Synth.* **1989**, *26*, 44.
(56) Hodgkinson, W. R.; Limpach, L. *J. Chem. Soc.* **1893**, *63*, 104.
(57) Stegmann, H. B.; Dumm, H. V.; Scheffer, K. *Phosphorus Sulfur* **1978**, *5*, 159.

[*i*-PrNON]Ti(*i*-Bu)$_2$. A solution of *i*-BuMgCl in ether (2.5 mL, 2.0 M) was added to a suspension of [*i*-PrNON]TiCl$_2$ (1.00 g, 2.49 mmol) in toluene (20 mL) at −25 °C. The mixture was rapidly stirred for 20 min without further cooling. 1,4-Dioxane (0.46 g, 5.2 mmol) was added, and the mixture was filtered through Celite. The filtrate was concentrated to ∼5 mL. Orange microcrystals began to form during the evaporation of the toluene. Pentane (5 mL) was added, and the mixture was stored at −25 °C overnight: yield 767 mg (69%); ^{1}H NMR δ 7.39 (d, 2), 6.92 (m, 4), 6.44 (t, 2), 5.99 (sept, 2, NC*H*Me$_2$), 2.03 (sept, 2, CH$_2$C*H*Me$_2$), 1.72 (d, C*H*$_2$CHMe$_2$), 1.70 (d, NCH*Me*$_2$, this and the previous resonance are not entirely resolved, overall integration 16), 0.66 (d, 12, CH$_2$CH*Me*$_2$); ^{13}C NMR (C$_6$D$_6$, 10 °C) δ 147.8, 145.3, 125.3, 115.7, 113.5, 112.8, 94.7 (*C*H$_2$CHMe$_2$), 50.7 (N*C*HMe$_2$), 32.2 (CH$_2$*C*HMe$_2$), 27.3 (CH$_2$CH*Me*$_2$), 20.2 (NCH*Me*$_2$). Anal. Calcd for C$_{26}$H$_{40}$N$_2$OTi: C, 70.26; H, 9.07; N, 6.30. Found: C, 70.12; H, 8.95; N, 6.38.

[*i*-PrNON]Ti(CH$_2$CMe$_3$)$_2$. A solution of Me$_3$CCH$_2$MgCl in ether (3.8 mL, 1.35 M) was added to a suspension of [*i*-PrNON]TiCl$_2$ (1.01 g, 2.52 mmol) in toluene (20 mL) at −25 °C. The solution was allowed to warm to room temperature. After 12 h 1,4-dioxane (0.46 g, 5.2 mmol) was added, and the mixture was filtered through Celite. The filtrate was concentrated to ∼5 mL, layered with pentane (10 mL), and stored at −25 °C. An orange-red microcrystalline solid was isolated: yield 606 mg (51%); ^{1}H NMR δ 7.31 (d, 2), 6.93 (m, 4), 6.43 (t, 2), 5.84 (sept, 2, C*H*Me$_2$), 2.04 (s, 4, C*H*$_2$CMe$_3$), 1.73 (d, 12, CH*Me*$_2$), 0.83 (s, 18, CH$_2$C*Me*$_3$); ^{13}C NMR δ 147.1, 145.9, 125.5, 115.7, 113.6, 113.4, 103.9 (*C*H$_2$CMe$_3$), 51.6 (*C*HMe$_2$), 38.7 (CH$_2$*C*Me$_3$), 34.5 (CH$_2$C*Me*$_3$), 21.0 (CH*Me*$_2$). Anal. Calcd for C$_{28}$H$_{44}$N$_2$OTi: C, 71.17; H, 9.39; N, 5.93. Found: C, 71.11; H, 9.32; N, 6.05.

[*i*-PrNON]ZrCl$_2$. H$_2$[*i*-PrNON] (3.02 g, 10.6 mmol) and Zr(NMe$_2$)$_4$ (2.84 g, 10.6 mmol) were dissolved in pentane (40 mL). The solution was stirred at room temperature for 3 h. All volatile components were removed in vacuo. Traces of HNMe$_2$ were removed by repeated trituration with pentane and gentle heating of the reaction flask. Proton and carbon NMR spectra of the pale yellow oil were consistent with it being (*i*-PrNON)Zr(NMe$_2$)$_2$: ^{1}H NMR δ 7.30 (d, 2), 7.02 (t, 2), 6.77 (d, 2), 6.43 (t, 2), 3.91 (sept, 2, C*H*Me$_2$), 2.78 (s, 12, N*Me*$_2$), 1.31 (d, 12, CH*Me*$_2$); ^{13}C NMR δ 148.0, 144.7, 126.4, 115.0, 113.8, 113.7, 51.2, 42.3, 23.9 (CH*Me*$_2$).

Toluene (40 mL) and Me$_3$SiCl (2.9 g, 26.7 mmol) were added to the oil. The solution quickly turned bright orange. After 14 h a small amount of solid was filtered off, and pentane (40 mL) was added to the filtrate. The layers were mixed, and the solution was then stored at −25 °C. A yellow, sometimes crystalline solid precipitated. The solid was filtered off and recrystallized from a mixture of toluene and pentane at −25 °C; yield 4.11 g (72%). According to ^{1}H NMR 1 equiv of toluene was present: ^{1}H NMR (CD$_2$Cl$_2$, toluene resonances not given) δ 7.67 (d, 2), 7.08 (t, 2), 6.83 (d, 2), 6.77 (t, 2), 4.66 (sept, 2, C*H*Me$_2$), 1.52 (d, 12, CH*Me*$_2$); ^{13}C NMR (CD$_2$Cl$_2$, toluene resonances not given) δ 148.2, 143.4, 126.1, 117.7, 114.7, 113.8, 48.9 (*C*HMe$_2$), 20.0 (CH*Me*$_2$). Anal. Calcd for C$_{25}$H$_{30}$Cl$_2$N$_2$OZr: C, 55.95; H, 5.63; N, 5.22. Found: C, 55.84; H, 5.61; N, 5.27.

[*i*-PrNON]ZrMe$_2$. A solution of MeMgI in ether (1.25 mL, 3.0 M) was added to a suspension of [*i*-PrNON]ZrCl$_2$ (1.01 g, 1.88 mmol) in toluene (20 mL) at −25 °C. The mixture was allowed to warm to room temperature and was stirred for 30 min. Dioxane (0.35 g, 4 mmol) was added, and the mixture was filtered through Celite. The pale yellow solution was concentrated to ∼5 mL and layered with pentane (∼10 mL). The mixture was stored at −25 °C overnight, and an off-white microcrystalline solid was isolated (565 mg, 74%): ^{1}H NMR δ 7.35 (d, 2), 6.92 (t, 2), 6.73 (d, 2), 6.41 (t, 2), 4.65 (m, 2, C*H*Me$_2$), 1.53 (d, 12, CH*Me*$_2$), 0.43 (s, 6, Zr*Me*$_2$); ^{13}C NMR δ 147.4, 144.8, 125.7, 115.3, 114.2, 113.0, 46.6 (*C*H*Me*$_2$), 41.6 (Zr*Me*$_2$), 21.0 (CH*Me*$_2$). Anal. Calcd for C$_{20}$H$_{28}$N$_2$OZr: C, 59.51; H, 6.99; N, 6.94. Found: C, 59.49; H, 6.87; N, 6.87.

An X-ray-quality crystal was obtained from a pentane solution at −25 °C.

[*i*-PrNON]ZrEt$_2$. A solution of EtMgBr in ether (700 μL, 3.0 M) was added to a solution of [*i*-PrNON]ZrCl$_2$ (562 mg, 1.05 mmol) in ether (30 mL) at −25 °C. After 5 min the yellow color disappeared, and a fine white precipitate formed. All volatile components were removed in vacuo. The residue was extracted with pentane (40 mL). The mixture was filtered through Celite, and the pale yellow filtrate was quickly concentrated to yield a light orange oil (∼1 mL). At −25 °C an off-white amorphous solid formed: yield 312 mg (69%); ^{1}H NMR δ 7.34 (d, 2), 6.93 (t, 2), 6.75 (d, 2), 6.41 (t, 2), 4.62 (br sept, 2, NC*H*Me$_2$), 1.54 (d, 12, NCH*Me*$_2$), 1.29 (t, 6, ZrCH$_2$C*H*$_3$), 0.91 (q, 4, ZrC*H*$_2$CH$_3$); ^{13}C NMR (tol-d_8, 0 °C) δ 147.0, 144.7, 115.1, 114.2, 113.1 (only 5 aromatic resonances were observed), 52.8 (t, J_{CH} = 115, ZrCH$_2$CH$_3$), 46.8 (N*C*HMe$_2$), 21.0 (NCH*Me*$_2$, overlapped with toluene signal), 11.1 (q, J_{CH} = 125, ZrCH$_2$*C*H$_3$). Anal. Calcd for C$_{22}$H$_{32}$N$_2$OZr: C, 61.21; H, 7.47; N, 6.49. Found: C, 61.28; H, 7.46; N, 6.51.

[*i*-PrNON]ZrPr$_2$. A 2.0 M solution of *n*-PrMgCl in ether (1.16 mL, 2.32 mmol) was added to a cooled (−30 °C) suspension of (*i*-PrNON)-ZrCl$_2$ (0.62 g, 1.16 mmol). The solution turned colorless, and a white precipitate formed. After 5 min the ether was removed in vacuo, and the residue was extracted with precooled (−30 °C) pentane. The extract was filtered through Celite, and the pentane was removed in vacuo. The residue was redissolved in 1−2 mL of pentane, and the solution was stored at −30 °C overnight to give large colorless crystals: yield 0.44 g (62%); ^{1}H NMR δ 7.34 (d, 2), 6.94 (t, 2), 6.78 (d, 2), 6.42 (t, 2), 4.72 (sept, 2, NC*H*Me$_2$), 1.69 (m, 4, ZrCH$_2$C*H*$_2$CH$_3$), 1.59 (d, 12, NCH*Me*$_2$), 1.01 (m, 4, ZrC*H*$_2$CH$_2$CH$_3$), 0.92 (t, 6, ZrCH$_2$CH$_2$C*H*$_3$); ^{13}C NMR δ 147.0, 144.8, 125.7, 115.1, 114.2, 113.3 (Aryl-C), 66.4 (ZrCH$_2$CH$_2$CH$_3$), 47.0 (N*C*HMe$_2$), 21.7 (NC*Me*$_2$), 21.2 (ZrCH$_2$*C*H$_2$CH$_3$), 20.5 (ZrCH$_2$CH$_2$CH$_3$). Anal. Calcd for C$_{24}$H$_{36}$N$_2$OZr: C, 62.70; H, 7.89; N, 6.09. Found: C, 62.59; H, 8.06; N, 6.05.

[*i*-PrNON]Zr(*i*-Bu)$_2$. Method A. A solution of *i*-BuMgCl in ether (1.9 mL, 2.0 M) was added to a suspension of [*i*-PrNON]ZrCl$_2$ (1.00 g, 1.86 mmol) in toluene (20 mL) at −25 °C. The mixture was allowed to warm to room temperature. Over a period of 30 min the yellow solid dissolved and was replaced by a fine white precipitate. 1,4-Dioxane (0.34 g, 3.86 mmol) was added, and the mixture was filtered through Celite. The pale yellow filtrate was concentrated to ∼5 mL, layered with pentane (10 mL), and stored at −25 °C. A colorless crystalline solid (713 mg) was isolated in two crops. Recrystallization from ether at −25 °C produced analytically pure material: yield 459 mg (51%); ^{1}H NMR δ 7.30 (d, 2), 6.93 (t, 2), 6.78 (d, 2), 6.40 (t, 2), 4.74 (br m, 2, NC*H*Me$_2$), 2.19 (sept, 2, CH$_2$C*H*Me$_2$), 1.61 (d, 12, NCH*Me*$_2$), 1.03 (d, 4, C*H*$_2$CHMe$_2$), 0.86 (d, 12, CH$_2$CH*Me*$_2$); ^{13}C NMR δ 146.8, 144.9, 125.8, 115.2, 114.2, 113.5, 76.6 (*C*H$_2$CHMe$_2$), 47.3 (N*C*HMe$_2$), 30.1 (CH$_2$*C*HMe$_2$), 28.5 (CH$_2$CH*Me*$_2$), 21.3 (NCH*Me*$_2$). Anal. Calcd for C$_{26}$H$_{40}$N$_2$OZr: C, 64.01; H, 8.26; N, 5.74. Found: C, 64.08; H, 8.14; N, 5.73.

Method B. A solution of H$_2$[*i*-PrNON] (1.39 g, 4.89 mmol) in toluene (10 mL) was added to a suspension of ZrCl$_4$ (1.14 g, 4.89 mmol) in toluene (40 mL) at room temperature. The mixture was stirred rapidly for 5 h. The thick slurry was cooled to −25 °C, and a solution of *i*-BuMgCl in ether (9.8 mL, 2.0 M) was added. After 30 min dioxane (1.73 g, 19.7 mmol) was added, and the mixture was filtered through Celite. All volatile components were removed in vacuo, leaving a dark solid residue. The solid was recrystallized twice from ether at −25 °C to give off-white microcrystals, yield 1.41 g (59%). The compound was identical in all respects to that prepared by method A.

[*i*-PrNON]Zr(CH$_2$CMe$_3$)$_2$. A solution of Me$_3$CCH$_2$MgCl in ether (2.8 mL, 1.35 M) was added to a suspension of [*i*-PrNON]ZrCl$_2$ (1.00 g, 1.86 mmol) in toluene (20 mL) at −25 °C. The mixture was allowed to warm to room temperature and stirred for 8 h. Dioxane (0.34 g, 3.86 mmol) was added, and the mixture was filtered through Celite. The pale yellow filtrate was concentrated to ∼3 mL and layered with pentane (8 mL). Pale yellow microcrystals began to form. The mixture was stored at −25 °C to complete crystallization: yield 673 mg (70%); ^{1}H NMR δ 7.20 (d, 2), 6.94 (t, 2), 6.78 (d, 2), 6.38 (t, 2), 4.70 (br m, 2, C*H*Me$_2$), 1.63 (d, 12, CH*Me*$_2$), 1.21 (s, 4, C*H*$_2$CMe$_3$), 0.97 (s, 18, CH$_2$C*Me*$_3$); ^{13}C NMR δ 146.3, 145.1, 126.0, 115.1, 114.3, 113.9, 84.6 (*C*H$_2$CMe$_3$), 48.1 (*C*HMe$_2$), 36.5 (CH$_2$*C*Me$_3$), 35.4 (CH$_2$C*Me*$_3$), 21.2 (CH*Me*$_2$). Anal. Calcd for C$_{28}$H$_{44}$N$_2$OZr: C, 65.19; H, 8.60; N, 5.43. Found: C, 65.36; H, 8.47; N, 5.41.

{[*i*-PrNON]Ti(PMe$_3$)$_2$}$_2$(μ-N$_2$). Inside a dinitrogen-filled drybox [*i*-PrNON]Ti(*i*-Bu)$_2$ (202 mg, 454 μmol) was dissolved in ether (20

mL) containing PMe_3 (145 mg, 1.91 mmol). The solution was transferred to a 100 mL one-neck flask which was then capped and allowed to stand at room temperature. The color changed gradually from bright orange to green black, and black crystals began to form. After 24 h the mixture was cooled to −25 °C to complete crystallization; yield 147 mg (61%). According to ^{1}H NMR 0.9 equiv of ether was present: ^{1}H NMR (C_6D_6, ether resonances not given) δ 7.14 (partially overlapped with C_6D_5H resonance), 6.99 (t, 4), 6.82 (d, 4), 6.35 (t, 4), 4.77 (br sept, 4, C*H*Me$_2$), 1.70 (d, 24, CH*Me*$_2$), 0.88 (d, 36, P*Me*$_3$, J_{PH} = 3.5); ^{13}C NMR (C_6D_6, ether resonances ignored) δ 149.3, 145.7, 125.8, 114.9, 112.8, 112.4, 54.2 (*C*HMe$_2$), 25.2 (CH*Me*$_2$) 15.3 (d, P*Me*$_3$, J_{PC} = 4.5); ^{31}P NMR δ −37.6. Anal. Calcd for $C_{51.6}H_{89}N_6O_3P_4Ti_2$: C, 58.49; H, 8.47; N, 7.93. Found: C, 58.35; H, 8.37; N, 7.86.

(*i*-PrNC$_6$H$_4$)(*i*-PrNC$_6$H$_4$O)Ti(dmpe). Inside a glovebox DMPE (71 mg, 473 μmol) was added to a suspension of [*i*-PrNON]Ti(*i*-Bu)$_2$ (201 mg, 452 μmol) in benzene (5 mL). The solid rapidly dissolved, and the solution began to darken within a few minutes. The solution was transferred to a 25 mL Schlenk tube which was then subjected to two freeze−pump−thaw cycles (120 mTorr of residual pressure). The reaction mixture was allowed to stand in the dark at room temperature. The color slowly changed to dark red-black. After 24 h the Schlenk tube was brought back into the glovebox, and all volatile components were removed in vacuo. The black residue was redissolved in a minimum of toluene (∼3 mL), concentrated to ∼1 mL, and layered with pentane (2 mL). The mixture was stored at −25 °C overnight to yield 137 mg (63%) of black crystals: ^{1}H NMR δ 7.32 (t, 1), 7.14 (partially overlapped with C_6D_5H), 6.90−6.85 (m, 3), 6.81 (t, 1), 6.74 (m, 1), 6.32 (m, 1), 4.05 (sept, 1, NC*H*Me$_2$), 3.92 (sept, NC*H*Me$_2$), 1.58 (d, 3), 1.3−0.8 (br m), 1.31 (d), 1.06 (d), 1.03 (d), 0.89 (d), total integration of previous peaks 22, 0.12 (br s, 3); ^{13}C NMR δ 173.9, 159.6, 154.3, 148.1, 130.3, 120.7, 119.5, 116.6 (t, $J_{CP} \approx 2$), 113.5, 108.3, 105.6 (11 aromatic resonances were observed), 53.3, 51.2, 27.2 (br s, DMPE), 26.3 (br s, DMPE), 25.1, 24.6, 24.3, 23.1, 12.7 (br s, DMPE), 11.8 (br s, DMPE), 10.8 (br s, DMPE); ^{31}P NMR δ −0.3 (br s), −8.6 (br s). Anal. Calcd for $C_{24}H_{38}N_2OP_2Ti$: C, 60.00; H, 7.97; N, 5.83. Found: C, 59.86; H, 7.91; N, 5.75.

[*i*-PrNON]Ti(CHCMe$_3$)(PMe$_3$)$_2$. A suspension of [*i*-PrNON]Ti(CH$_2$CMe$_3$)$_2$ (300 mg, 635 μmol) in toluene (6 mL) and PMe_3 (0.60 g, 7.9 mmol) was stirred in a sealed 50 mL Schlenk tube at 45 °C. The solid quickly dissolved, and the initially bright orange solution turned green-black within a few hours. After 12 h the solution was concentrated to ∼1 mL. Black crystals began to form during the evaporation of the toluene. More PMe_3 (∼150 mg) was added, and the mixture was stored at −25 °C overnight to afford black crystals; yield 178 mg (51%). Shifts in ^{1}H and ^{13}C NMR spectra vary slightly depending on the concentration of the sample: ^{1}H NMR (0.06 M in C_6D_6) δ 7.12 (d, 2), 6.90 (t, 2), 6.67 (d, 2), 6.33 (t, 2), 4.97 (br m, 2, NC*H*Me$_2$), 3.00 (s, 1, C*H*CMe$_3$), 1.62 (d, 12, NCH*Me*$_2$), 1.20 (s, 9, CHC*Me*$_3$), 0.90 (d, J_{PH} = 4, 18, PMe$_3$); ^{13}C NMR (0.06 M in C_6D_6) δ 230.1 (in gated decoupled ^{13}C, d, J_{CH} = 80, *C*HCMe$_3$), 149.1, 144.9, 125.1, 113.8, 113.5, 112.6, 53.2 (N*C*HMe$_2$), 47.6 (CH*C*Me$_3$), 33.8, 24.3, 16.5 (P*Me*$_3$); ^{31}P NMR (0.06 M in C_6D_6) δ −30.9 (br s). Anal. Calcd for $C_{29}H_{50}N_2OP_2Ti$: C, 63.04; H, 9.12; N, 5.07. Found: C, 63.12; H, 8.98; N, 5.20.

{[*i*-PrNON]ZrEt}$_2$(μ-C$_2$H$_4$). [*i*-PrNON]ZrEt$_2$ (239 mg, 554 μmol) was dissolved in pentane (6 mL). The sometimes slightly cloudy solution was filtered and allowed to stand at room temperature. During the reaction the color changed from very pale yellow to red-orange. After a few hours pale yellow needles began to form. After 21 h the supernatant was decanted off, and the solid was washed liberally with pentane and dried in vacuo; yield 173 mg (75%). The product is contaminated with traces (∼2% by ^{1}H NMR) of [*i*-PrNON]ZrEt$_2$. A sample free of [*i*-PrNON]ZrEt$_2$ may be obtained as a yellow powder from a saturated toluene solution layered with ether: ^{1}H NMR δ 7.47 (d, 4), 6.95 (t, 4), 6.76 (d, 4), 6.49 (t, 4), 3.75 (sept, 4, NC*H*Me^{A}Me^B), 1.45 (t, 6, ZrCH$_2$C*H*$_3$), 1.38 (d, 12, NCH*Me*^{A}Me^B), 1.29 (d, 12, NCHMe^A*Me*^{B}), 1.16 (q, 4, ZrC*H*$_2$CH$_3$), 1.09 (s, 4, μ-C$_2$*H*$_4$); ^{13}C NMR δ 146.7, 144.8, 125.5, 115.6, 114.5, 114.2, 46.3 (N*C*HMe^{A}Me^B), 44.7 (t, J_{CH} = 117, ZrCH$_2$CH$_3$), 39.4 (t, J_{CH} = 143, μ-*C*$_2$H$_4$), 21.7 (NCH*Me*^{A}-Me^B), 20.9 (NCHMe^A*Me*^{B}), 13.0 (q, J_{CH} = 124, ZrCH$_2$*C*H$_3$). Anal. Calcd for $C_{42}H_{58}N_4O_2Zr_2$: C, 60.53; H, 7.01; N, 6.72. Found: C, 60.19; H, 6.95; N, 6.73.

[*i*-PrNON]Zr(*i*-Bu)$_2$(PMe$_3$). PMe_3 (93 mg, 1.22 mmol) was added to a suspension of [*i*-PrNON]Zr(*i*-Bu)$_2$ (209 mg, 428 μmol) in pentane (5 mL) at room temperature. The solid rapidly dissolved, and the color changed to pale yellow. The solution was concentrated to ∼1 mL. Pale yellow microcrystals began to form. More PMe_3 (100 mg, 1.32 mmol) was added, and the mixture was stored at −25 °C overnight. The supernatant was decanted off, and the solid was rinsed with a little pentane and dried in vacuo: yield 115 mg (48%); ^{1}H NMR (∼0.013M in C_6D_6) δ 7.31 (d, 2), 6.92 (t, 2), 6.78 (d, 2), 6.40 (t, 2), 4.78 (br s, 2, NC*H*Me$_2$), 2.20 (sept, 2, CH$_2$C*H*Me$_2$), 1.61 (d, 12, NCH*Me*$_2$), 1.03 (d, 4, C*H*$_2$CHMe$_2$), 0.88 (d, 12, CH$_2$CH*Me*$_2$), 0.74 (d, 9, P*Me*$_3$, J_{PH} = 2); ^{1}H NMR (∼0.13 M in C_6D_6) δ 7.32 (d, 2), 6.90 (t, 2), 6.76 (d, 2), 6.39 (t, 2), 4.89 (br s, 2), 2.24 (sept, 2), 1.61 (d, 12), 1.01 (d, 4), 0.95 (d, 12, CH$_2$CH*Me*$_2$), 0.63 (s, 9, P*Me*$_3$); ^{13}C NMR (∼0.13 M in C_6D_6) δ 146.7, 145.1, 125.7, 115.0, 114.1, 113.6, 76.1 (*C*H$_2$CHMe$_2$), 46.8 (N*C*HMe$_2$), 30.5 (CH$_2$*C*HMe$_2$), 28.8 (CH$_2$CH*Me*$_2$), 21.3 (NCH*Me*$_2$), 15.8 (d, P*Me*$_3$, J_{PC} = 8); ^{31}P NMR (∼0.13 M in C_6D_6) δ −57.2. Anal. Calcd for $C_{29}H_{49}N_2OPZr$: C, 61.77; H, 8.76; N, 4.97. Found: C, 61.82; H, 8.62; N, 5.01.

[*i*-PrNON]Zr(η^2-CH$_2$CMe$_2$)(PMe$_3$)$_2$. A solution of [*i*-PrNON]Zr(*i*-Bu)$_2$ (303 mg, 621 μmol) in PMe_3 (2.5 g, 32.9 mmol) was heated in a sealed 25 mL Schlenk tube to 37 °C in the dark. After 63 h the solution had turned red and was transferred into a 20 mL vial. Needles began to form immediately. Ether (∼1 mL) was added, and the mixture was stored at −25 °C overnight. The supernatant was decanted off, and the solid was washed with pentane to give pink-brown needles (185 mg). The washings were combined, concentrated, and stored at −25 °C to give a second crop (29 mg) as a powder: overall yield 214 mg (59%); ^{1}H NMR δ 7.38 (d, 2), 6.82 (t, 2), 6.61 (d, 2), 6.40 (t, 2), 3.43 (sept, 2, NC*H*Me^{A}Me^B), 1.94 (s, 6, CH$_2$C*Me*$_2$), 1.23 (d, 6, NCH*Me*^{A}Me^B), 1.17 (d, 6, NCHMe^A*Me*^{B}), 0.96 (s, C*H*$_2$CMe$_2$), 0.93 (br s, P*Me*$_3$), 0.86 (br s, P*Me*$_3$ previous 3 peaks overlapped, overall integration 20); ^{13}C NMR δ 147.0, 146.1, 124.6, 115.8, 113.9, 113.6, 63.6 (*C*H$_2$CMe$_2$), 52.3 (CH$_2$*C*Me$_2$), 44.2 (N*C*HMe^{A}Me^B), 34.2 (CH$_2$C*Me*$_2$), 22.6 (NCH*Me*^{A}Me^B), 22.4 (NCHMe^A*Me*^{B}), 16.3 (br s, P*Me*$_3$), 15.5 (br s, P*Me*$_3$); ^{31}P NMR δ −26.0 (br s), −60.1 (br s). Anal. Calcd for $C_{28}H_{48}N_2OP_2Zr$: C, 57.80; H, 8.31; N, 4.81. Found: C, 57.63; H, 8.24; N, 4.72.

[*i*-PrNON]Zr(η^2-C$_2$H$_4$)(PMe$_3$)$_2$. [*i*-PrNON]ZrEt$_2$ (13 mg, 0.03 mmol) was dissolved in 0.5 mL of C_6D_6, and PMe_3 (5 mg, 0.07 mmol) was added. The solution was transferred to a NMR tube, and the ^{1}H and ^{13}C NMR spectra were recorded: ^{1}H NMR δ 7.42 (d, 2), 6.88 (t, 2), 6.47 (d, 2), 6.43 (t, 2), 3.07 (sept, 2, NC*H*Me$_2$), 1.20 (s, C$_2$*H*$_4$), 0.97 (d, 12, NCH*Me*$_2$), 0.90 (s, 18, P*Me*$_3$); ^{13}C NMR δ 147.7, 145.7, 125.1, 113.9, 113.7, 113.3 (C$_{Ar}$), 45.7 (C$_2$H$_4$), 44.0 (N*C*HMe$_2$), 21.6 (NCH*Me*$_2$), 15.1 (br, P*Me*$_3$). No further products besides C_2H_6 (δ = 0.80) could be observed.

[*i*-PrNON]Zr(η^2-CH$_2$CHMe)(PMe$_3$)$_2$. [*i*-PrNON]ZrPr$_2$ (32 mg, 0.07 mmol) was dissolved in 0.5 mL of C_6D_6, and PMe_3 (11 mg, 0.14 mmol) was added. The solution was transferred to a NMR tube, and a ^{1}H NMR spectrum was recorded. After 20 min, starting material, product, and propane resonances could be observed. After the reaction was complete (3 h), the solution was frozen and all volatile components were removed in vacuo: ^{1}H NMR δ 7.40 (m, 2), 6.86 (m, 2), 6.59 (d, 1), 6.48 (d, 1), 6.41 (m, 2). 3.16 (sept, 1, NC*H*Me$_2$), 3.00 (sept, 1, NC*H*Me$_2$), 2.18 (d, ^3J = 6.5, 3, CH$_2$=CH*Me*), 1.56 (dd, ^3J = 9 and 13, 1, CH$_2$C*H*Me), 1.17 (d, 1, NCH*Me*$_2$), 1.12 (d, 1, NCH*Me*$_2$), 1.06 (d, 1, NCH*Me*$_2$), 1.02 (d, 1, NCH*Me*$_2$), 0.88 (s, br, ∼18, P*Me*$_3$), 0.75 (dd, ^3J = 9 and 11, 1, C*H*$_2$CHMe); the resonance of one olefinic proton could not be detected and is probably buried under the broad PMe_3 resonance; ^{13}C NMR δ 147.4, 147.3, 146.1, 145.5, 125.0, 124.8, 114.8, 114.5, 114.2, 113.3, 113.2, 113.0 (C$_{Ar}$), 53.3 (CH$_2$=*C*HMe), 52.0 (*C*H$_2$=CHMe), 46.4 (N*C*HMe$_2$), 44.1 (N*C*HMe$_2$), 26.5 (CH$_2$=CH*Me*), 24.1 (NCH*Me*$_2$), 22.7 (NCH*Me*$_2$), 21.6 (NCH*Me*$_2$), 21.5 (NCH*Me*$_2$), 15.4 (br, P*Me*$_3$). No other products were observed.

H$_2$[CyNON]. To a 250 mL round-bottom one-necked flask equipped with a condenser and charged with a Teflon-sealed stir bar were added O(*o*-C$_6$H$_4$NH$_2$)$_2$ (5.03 g, 0.025 mol), cyclohexanone (4.93 g, 0.050 mol, 2 equiv), zinc (16.42 g, 0.25 mol, 10 equiv), and acetic acid (100 mL). The mixture was heated to 65 °C under nitrogen for 29 h. The gray-white suspension containing residual zinc was cooled to room tem-

perature, and methanol (100 mL) was added. The white precipitate was filtered off, and the filter cake was washed with MeOH (100 mL). The filtrate and combined washings were concentrated on a rotary evaporator to ~10 mL, and crushed ice (~100 g) and CH_2Cl_2 (100 mL) were added. Ammonium hydroxide was then added until pH > 10. The organic layer was separated from the aqueous layer, which was further washed with CH_2Cl_2 (100 mL). The combined organic solutions were dried over $MgSO_4$, and the solvent was removed under reduced pressure to give the product as a yellow oil which was pure by NMR and used for subsequent organometallic chemistry without further purification: yield 8.03 g (88%); ^{1}H NMR δ 6.99 (t, 2, Ar), 6.93 (d, 2, Ar), 6.71 (d, 2, Ar), 6.59 (t, 2, Ar), 4.29 (s, 2, NH), 3.15 (m, 2, Cy), 1.88 (m, 4, Cy), 1.49 (m, 4, Cy), 1.39 (m, 2, Cy), 1.12 (m, 4, Cy), 0.95 (m, 6, Cy); ^{1}H NMR ($CDCl_3$) δ 6.99 (t, 2, Ar), 6.76 (m, 4, Ar), 6.59 (t, 2, Ar), 4.19 (br s, 2, NH), 3.32 (m, 2, Cy), 2.08 (m, 4, Cy), 1.77−1.63 (m, 6, Cy), 1.44−1.16 (m, 10, Cy); ^{13}C NMR ($CDCl_3$) δ 143.98 (C, Ar), 139.12 (C, Ar), 124.33 (CH, Ar), 118.02 (CH, Ar), 116.27 (CH, Ar), 11.92 (CH, Ar), 51.54 (CH, Cy), 33.46 (CH_2, Cy), 26.07 (CH_2, Cy), 25.09 (CH_2, Cy); HRMS (EI, 70 eV) 364.25132, calcd for $C_{24}H_{32}N_2O$ 364.251464.

The synthetic procedures for $[CyNON]^{2-}$ complexes are analogous to those for $[i\text{-PrNON}]^{2-}$ complexes. Syntheses and spectroscopic details can be found in the Supporting Information for [CyNON]Ti(NMe_2)$_2$, [CyNON]$TiCl_2$, [CyNON]$TiMe_2$, [CyNON]Ti(CH_2CMe_3)$_2$, [CyNON]Ti(*i*-Bu)$_2$, [CyNON]Zr(NMe_2)$_2$, [CyNON]$ZrCl_2$, [CyNON]Zr(CH_2SiMe_3)$_2$, [CyNON]$ZrMe_2$, [CyNON]Zr(CH_2CMe_3)$_2$, [CyNON]$ZrEt_2$, [CyNON]Zr(*i*-Bu)$_2$, [CyNON]Zr($CH_2CH{=}CH_2$)$_2$, [CyNON]Zr(η^2-C_2H_4)(PMe_3)$_2$, and [CyNON]Zr(η^2-H_2CCMe_2)(PMe_3)$_2$.

{[CyNON]ZrMe(NMe$_2$Ph)}{B(C$_6$F$_5$)$_4$} Cation Observation. A cold solution (−35 °C) of $[CyNON]ZrMe_2$ (10 mg, 0.021 mmol) in bromobenzene-d_5 (0.7 mL) was added to solid $[HNMe_2Ph][B(C_6F_5)_4]$ (17 mg, 0.021 mmol) at −35 °C. The color changed from colorless to yellow immediately, and then turned yellow-orange in ~30 s. The solution was stirred at room temperature briefly, and was then cooled to −35 °C again before being transferred to a Teflon-sealed NMR tube, which was then frozen in liquid nitrogen. Proton spectra were acquired at several temperatures starting at −30 °C. The spectra were essentially the same between −30 and +20 °C: ^{1}H NMR (C_6D_5Br, 0 °C) δ 7.24 (d, 2, Ar), 7.19 (t, 2, Ar), 7.00 (m, 3, Ar), 6.75 (d, 2, Ar), 6.68 (m, 4, Ar), 3.37 (tt, 2, Cy), 2.49 (s, 6, N*Me*$_2$Ph), 1.85 (m, 4, Cy), 1.73 (m, 4, Cy), 1.58 (m, 4, Cy), 1.23 (m, 2, Cy), 1.07 (m, 6, Cy), 0.65 (s, 3, Zr*Me*).

Catalytic Reaction between {[CyNON]ZrMe(NMe$_2$Ph)}{B(C$_6$F$_5$)$_4$} and 1-Hexene. {[CyNON]ZrMe(NMe_2Ph)}{$B(C_6F_5)_4$} was prepared by the above method. To a solution of {[CyNON]ZrMe(NMe_2Ph)}{$B(C_6F_5)_4$} in bromobenzene-d_5 at 0 °C was added 50 equiv of 1-hexene. The solution was transferred to an NMR tube and kept at 0 °C. The reaction was monitored by ^{1}H NMR.

X-ray Structures. A Siemens SMART/CCD area detection system with Mo Kα radiation (λ = 0.710 73 Å) was used for all determinations. Cell determination, data collection, and structure solution and refinement were performed with the SMART SAINT and SHELXTL 5.0 software packages. All non-hydrogen atoms were refined anisotropically, and all hydrogen atoms were placed in calculated positions. {[*i*-PrNON]Ti(PMe_3)$_2$}$_2$(μ-N_2) contained disordered ether which was removed during the refinement procedure using the SQUEEZE[58] routine. During the refinement of [*i*-PrNON]Ti(CH_2CHMe_2)$_2$ it appeared that the isobutyl methyne carbons (C(2) and C(6)) were disordered over two positions close to one another. Subsequent refinement led to collapse of the two positions to the one position, which is the one that is reported. The *tert*-butyl group in [*i*-PrNON]Ti($CHCMe_3$)(PMe_3)$_2$ was found to be disordered rotationally over two equally populated positions and was refined as such. All six methyl carbon atom positions are listed in the table of positional parameters in the Supporting Information.

Acknowledgment. R.R.S. is grateful to the National Institutes of Health (Grant GM 31978) and the National Science Foundation (Grant CHE-9700736) for research support. We also thank Dr. David McConville for disclosing results prior to publication and for fruitful discussions. R.B. thanks the Studienstiftung des Deutschen Volkes for a predoctoral fellowship, while R.S. thanks the Alexander von Humboldt Foundation for a Feodor-Lynen-Fellowship.

Supporting Information Available: Experimental details for the synthesis of $[CyNON]^{2-}$ complexes, along with ORTEP drawings, crystal data, atomic coordinates, bond lengths and angles, and anisotropic displacement parameters for [*i*-PrNON]Ti(CH_2CHMe_2)$_2$ (**1**), [*i*-PrNON]$ZrMe_2$ (**2**), [*i*-PrNON]Zr(CH_2CHMe_2)$_2$(PMe_3) (**3**), [*i*-PrNON]Zr(CH_2CMe_2)(PMe_3)$_2$ (**4**), [*i*-PrNON]Ti(PMe_3)$_2$]$_2$(μ-N_2) (**5**), (*i*-PrNC_6H_4)(*i*-PrNC_6H_4O)Ti(dmpe) (**6**), and [*i*-PrNON]Ti($CHCMe_3$)(PMe_3)$_2$ (**7**) (PDF). This material is available free of charge via the Internet at http://pubs.acs.org.

JA983549V

(58) van der Sluis, P.; Spek, A. L. *Acta Crystallogr.* **1990**, *A46*, 194.